ON THE MAGNITUDE OF DARK ENERGY VOIDS AND OVERDENSITIES

David F. Mota[1], Douglas J. Shaw[2] and Joseph Silk[3]

[1] Institute for Theoretical Physics, University of Heidelberg, 69120 Heidelberg, Germany
[2] DAMTP, Centre for Mathematical Sciences, University of Cambridge, Cambridge CB3 0WA, UK and
[3] Astrophysics, University of Oxford, Oxford OX1 3RH, UK

Draft version February 1, 2008

ABSTRACT

We investigate the clustering of dark energy within matter overdensities and voids. In particular, we derive an analytical expression for the dark energy density perturbations, which is valid both in the linear, quasi-linear and fully non-linear regime of structure formation. We also investigate the possibility of detecting such dark energy clustering through the ISW effect. In the case of uncoupled quintessence models, if the mass of the field is of order the Hubble scale today or smaller, dark energy fluctuations are always small compared to the matter density contrast. Even when the matter perturbations enter the non-linear regime, the dark energy perturbations remain linear. We find that virialised clusters and voids correspond to local overdensities in dark energy, with $\delta_\phi/(1+w) \sim \mathcal{O}(10^{-5})$ for voids, $\delta_\phi/(1+w) \sim \mathcal{O}(10^{-4})$ for super-voids and $\delta_\phi/(1+w) \sim \mathcal{O}(10^{-5})$ for a typical virialised cluster. If voids with radii of $100-300\,\mathrm{Mpc}$ exist within the visible Universe then δ_ϕ may be as large as $10^{-3}(1+w)$. Linear overdensities of matter and super-clusters generally correspond to local voids in dark energy; for a typical super-cluster: $\delta_\phi/(1+w) \sim \mathcal{O}(-10^{-5})$. The approach taken in this work could be straightforwardly extended to study the clustering of more general dark energy models.

Subject headings: Cosmology: Theory, miscellaneous. Relativity. Galaxies: general, Large scale structure of the universe.

1. INTRODUCTION

It has been almost a decade since observations of Type Ia supernovae (SNe Ia) were first found to support the notion that our universe is currently undergoing a phase of accelerated expansion (Riess et al. 1998; Perlmutter et al. 1999). Since that time, evidence in favour of this accelerated expansion has strengthened significantly as the result of further SNe Ia observations (Riess et al. 2004, 2006a,b; Wood-Vasey et al. 2007), improved measurements of the cosmic microwave background (CMB) (Spergel et al. 2003, 2007) and surveys of large scale structure (LSS) (Adelman-McCarthy et al. 2006; Tegmark et al. 2006). The precise cause of this late-time acceleration, however, remains unknown.

If general relativity is accurate on astrophysical scales, then the assumptions of large-scale homogeneity and isotropy require that the agent responsible for the universe's acceleration, dubbed 'dark energy', behave cosmologically as a fluid with negative pressure. The standard model of particle physics predicts only one such fluid: the vacuum energy, or cosmological constant, for which the pressure, p, is always equal to minus the energy density, ρ. However, if the vacuum energy density is indeed non-zero then it is generally expected to be of the order of M_{Pl}^4, where M_{Pl} is the Planck-mass. This is some 120 orders of magnitude larger than the observed dark energy density. A number of proposals have therefore been made in the literature for models in which dark energy is dynamical and associated with some new form of energy (Wetterich 1988; Peebles & Ratra 1988). In these models, the present small size of the effective cosmological constant is by-product of the age of Universe. The acceleration of the Universe might alternatively be explained by modifying General Relativity rather than postulating

a new form of energy (see Dvali, Gabadadze & Porrati 2000; Amarzguioui et al. 2006; Nojiri & Odintsov 2003; Capozziello, Cardone & Troisi 2005; Koivisto & Mota 2007a,b). It also been suggested that the Universe is not accelerating at all, but that a large local inhomogeneity prevents the SNe Ia data from being correctly interpreted in terms of a homogeneous and isotropic cosmological model (Kolb Matarrese & Riotto 2006; Moffat 2006). This said, dynamical dark energy (hereafter DDE) is by far the most popular candidate to explain the current astronomical data. In the simplest DDE models, known as quintessence, dark energy is associated with the energy density of a scalar field with a canonical kinetic structure.

If dark energy does indeed exist then astronomical observations presently provide us with only hints as to its nature. We know that today it represents about 70% of the total energy density of the Universe, and that its equation of state (EoS) parameter, $w \equiv p/\rho$, is fairly close to -1: $w = -1 \pm 0.1$ for $z < 1$, (Riess et al. 2006a). Furthermore, if matter dominates the expansion of the Universe for $z > 1.8$ then $w(z > 1) = -0.8^{+0.6}_{-0.1}$ (Riess et al. 2006a). Hence, dark energy has negative pressure at higher redshifts with a 98% confidence. These bounds on w are entirely consistent with a pure cosmological constant. Whilst detecting either $w \neq -1$ or $\mathrm{d}w/\mathrm{d}z \neq 0$ would rule out a cosmological constant, in many DDE models significant deviations from $w = -1$ only occur at early times and as such would be difficult to detect. The late time, background cosmology predicted by many DDE models is therefore very similar to that of a universe with a true cosmological constant.

DDE models generally cease to mimic a cosmological constant in inhomogeneous backgrounds or when one considers cosmological perturbation the-

ory. In particular, a number of authors have studied the effect of DDE on the formation of large scale structure (Corasaniti, Giannantonio & Melchiorri 2005; Hannestad & Mortsell 2002; Brookfield et al. 2006b; Doran, Robbers & Wetterich 2007). In the vast majority of these works the energy density of dark energy is taken to be homogeneous i.e. it is assumed that DDE does *not* cluster. The extent to which this assumption of homogeneity is valid has been the subject of some interest and much debate in the literature. In an inhomogeneous background, the DDE energy density and EoS parameter should exhibit some spatial variations. The key issue of how large these variations should be is however far from settled, particularly when the matter perturbation goes non-linear (Maor & Lahav 2005; Mota & van de Bruck 2004; Linder & White 2005; Bartelmann, Doran & Wetterich 2005; Nunes & Mota 2006; Abramo et al. 2007). In this paper we attempt to settle this issue for uncoupled quintessence models by deriving an analytical expression for the dark energy contrast, δ_ϕ, in by presence of a matter perturbation. Importantly, we do *not* constrain the matter perturbation to be small (i.e. linear).

Clustering of DDE over scales smaller than about 100 Mpc has been the subject of a number of recent articles (Caimmi 2007; Balaguera-Antolínez, Mota & Nowakowski 2006; Mainini 2005; Percival 2005; Wang 2006; Nunes, da Silva & Aghanim 2005; Balaguera-Antolínez, Mota & Nowakowski 2007). Most attention has been focussed on models in which the DDE couples to baryonic and/or dark matter since DDE clustering is expected to be strongest in such theories (Amendola 2000; Brookfield et al. 2006a; Manera & Mota 2006; Pettorino, Baccigalupi & Mangano 2005). In other works, a more phenomenological approach has been taken and the observables associated with DDE clustering have been parametrized. In particular, it has been shown that inhomogeneities in dark energy could produce detectable signatures on the CMB (Weller & Lewis 2003; Koivisto & Mota 2006).

Recently, Dutta & Maor (2007) considered the growth of spatial DDE perturbations in the *absence* of any matter coupling. They considered only those circumstances where both the density contrast of matter, δ_m, and that of the DDE, δ_ϕ, were small enough to be treated as a linearized perturbations about a homogeneous and isotropic cosmological background. They studied the simplest class of quintessence models where dark energy is associated with the slow-roll of a scalar field ϕ down a potential $V(\phi)$; ϕ is minimally coupled to gravity. The authors linearized the full field equations for ϕ, the matter and the metric and solved the resulting system numerically. Intriguingly they found that, at late times, a local overdensity of matter corresponded to a local under-density, or void, of dark energy. Conversely, a void in the matter was seen to produce a local DDE overdensity. Although the DDE density contrast, δ_ϕ, is initially very small compared to the matter density contrast, δ_m, they found that, when $\delta_m \sim \mathcal{O}(1)$, $|\delta_\phi| \sim \mathcal{O}(10^{-2})$. δ_ϕ was also observed to be growing more quickly than δ_m at late times. Their results suggest that DDE clustering may induce a positive correction to the value of $(1+w)$ of more than 10% at the centre of an inhomogeneity with properties similar to that of the local supercluster (hereafter LSC). If accurate, the results of Dutta & Maor (2007) imply that any deviations from $w = -1$ would be significantly amplified by the presence of a local overdensity of matter. Furthermore, they suggest that DDE clustering might be relatively strong when the matter perturbation goes non-linear.

Dutta & Maor (2007) studied DDE clustering when the matter perturbation is growing in the linear regime, which is only accurate when $\delta_m \ll 1$. They considered the evolution δ_ϕ for a cluster of matter with initial density profile (at $z = 35$) of $\delta_m = A \exp(-r^2/\sigma^2)$ where $A = 0.1$ and $\sigma = 0.01 H_i^{-1}$ with H_i being the initial value of the Hubble parameter. However, in the absence of any DDE, the linear approximation would generally cease to be accurate when $z \approx 2.8$; additionally the perturbation would be expected to turnaround when $z \approx 1.0$ and virialise when $z \approx 0.3$. It is therefore far from clear whether or not the sharp late-time growth in δ_ϕ found by Dutta & Maor (2007) is indeed a physical effect, or just a result of using linearized field equations outside of realm in which they are valid. Although one might well expect there exist some mapping between the linear and non-linear regimes as it happens in an Einstein-de Sitter Universe.

In this paper we investigate a similar problem to that considered by Dutta & Maor (2007), i.e. the clustering of uncoupled quintessence on sub-horizon scales. There are, however, two important differences between our approach to this problem and the one taken by Dutta & Maor (2007):

1. Firstly, we do *not* use numerical simulations but instead use the method of matched asymptotic expansions (MAEs) to develop a analytical approximation to δ_ϕ.

2. Secondly, we do *not* require the density contrast of the matter perturbation, δ_m, to be small. Indeed, our analysis and results remain valid even after the virialisation of the matter overdensity.

Our approximation for δ_ϕ is accurate provided that δ_m is only non-linear ($\gtrsim \mathcal{O}(1)$) on sub-horizon scales. This provision is consistent with observations. For simplicity we take the matter perturbation to be spherical symmetric. We also require that gravity is suitably weak whenever the inhomogeneity is non-linear i.e. $GM/R \ll 1$. We restate these requirements in a rigorous fashion later, however they are essentially equivalent to the statement that gravity is approximately Newtonian over scales smaller than H^{-1}. Since DDE clustering in the linear regime has been dealt with in great detail by Dutta & Maor (2007), our main focus in this paper is on what occurs when the matter perturbation goes non-linear.

This paper is organized as follows: in Section 2 we describe our model for an inhomogeneous spacetime and the DDE. We state the equations that must be satisfied by the metric quantities and the dark energy scalar field ϕ. In Section 3 we introduce the method of matched asymptotic expansions (MAEs). This method relies the existence of locally small parameters, and we state what these are for our model and interpret them physically.

We also note what constraints the smallness of these parameters places upon our analysis. In Section 4 we apply the method of MAEs to the evolution of dynamical dark energy perturbations. We derive a simple equation for the DDE density contrast, δ_ϕ, in terms of the peculiar velocity of matter particles, δv, and the matter density contrast, δ_m. Importantly this equation is equally as valid for $\delta_m \gtrsim \mathcal{O}(1)$ ('the non-linear regime') as it is when $\delta_m \ll \mathcal{O}(1)$ ('the linear regime'). In Section 5 we use our results to study the evolution of δ_ϕ in the linear ($\delta_m \ll 1$), quasi-linear ($\delta_m \sim \mathcal{O}(1) - \mathcal{O}(10)$) and fully non-linear ($\delta_m \gg 1$) regimes. We compare our analytical results with those found numerically in the linear regime by Dutta & Maor (2007). In Section 6 we consider the spatial profile of the DDE density contrast for realistic astrophysical inhomogeneities such as voids, supervoids, clusters and superclusters. We conclude in Section 7 with a discussion of our results and their observational implications. We also note how our analysis might be extended to include even more general DDE models.

Throughout the paper we use units where $c = 1$.

2. THE MODEL

2.1. *Geometrical Set-Up*

Our aim in this paper is to derive an expression for the DDE density contrast, $\delta_\phi = \delta \varepsilon^{(\phi)}/\varepsilon_c^{(\phi)}$, inside an over-density, or under-density, of matter. Henceforth we use $\varepsilon^{(i)}$ to represent the energy density of a component i. We are particularly interested in those cases where the matter perturbation is non-linear i.e. $\delta \varepsilon^{(m)}/\varepsilon_c^{(m)} \gtrsim \mathcal{O}(1)$. Although we aim to remain suitably general in our treatment of the density perturbation, we do make the following simplifying assumptions:

- We assume spherical symmetry. We briefly discuss the extent to which the relaxation of this assumption would affect our results in Section 7 below, and conclude that the qualitative nature of our findings would be unaffected.

- We define a 'physical radial coordinate', R, by the requirement that a spherical surface with physical radius R has surface area $4\pi R^2$. We assume that all curvature invariants are regular at $R = 0$ i.e. we do not consider those cases in which there is a central black hole. We argue below, however, that our results are still accurate even when there is a central black-hole, provided they are only applied at radii that are large compared to the Schwarzschild radius of the black hole.

- Finally we assume that for radii smaller than some $R_0 \ll H^{-1}$ gravity is suitably *weak* in the inhomogeneous region; H is the Hubble parameter of the background spacetime. We define what we mean by *weak* rigorously in Section 3. For radii $R > R_0$, we require that the matter density contrast is $\lesssim 1$. This assumption holds for most realistic models of collapsing overdensities provided that the radius the overdense region is less than about $0.1/H$.

2.2. *Einstein's Equations*

We take the matter content of the Universe to be a mix of irrotational dust and dynamical dark energy, which is described by a scalar field ϕ. For simplicity we restrict ourselves to considering only spherically symmetric spacetimes for which the most general line element in comoving coordinates is:

$$\mathrm{d}s^2 = \mathrm{d}t^2 - U(t,r)\,\mathrm{d}r^2 - R(t,r)^2 \left(\mathrm{d}\theta^2 + \sin^2\theta\,\mathrm{d}\varphi^2 \right).$$

We make the definitions $U(t,r) \equiv R_{,r}^2(t,r)/Q(t,r)$ and $k(t,r) \equiv 1 - Q(r,t)$. This coordinate choice is unique up to $t \to t + t_0$, and $r \to r'(r)$. With these definitions the 2-spheres $\{t,r\} = \mathrm{const}$ have surface area $4\pi R^2(t,r)$, and in this sense $R(t,r)$ represents the 'physical radial coordinate'. The energy-momentum tensor of pressureless dust is given by

$$T_{ab}^{(m)} = \mathrm{diag}\left(\varepsilon^{(m)}, 0, 0, 0 \right),$$

and the energy-momentum tensor of the scalar field, ϕ, is

$$T_{ab}^{(\phi)} = \partial_a\phi\partial_b\phi - g_{ab}\left(\frac{1}{2}\partial_c\phi\partial^c\phi - V(\phi) \right).$$

The Einstein equations for this metric read:

$$G_{ab} = R_{ab} - \frac{1}{2}Rg_{ab} = \kappa\left(T_{ab}^{(m)} + T_{ab}^{(\phi)} \right), \qquad (1)$$

where $\kappa = 8\pi$. The tt-component of Eq. (1) gives:

$$\left(R_{,t}^2 R + kR \right)_{,r} = R_{,r}R^2\kappa\varepsilon^{(m)} + R_{,r}R^2\kappa\left(\frac{1}{2}\dot\phi^2 \right. \qquad (2)$$

$$\left. + \frac{Q}{2R_{,r}^2}\phi_{,r}^2 + V(\phi) \right) + RR_{,r}R_{,t}\frac{\dot Q}{Q},$$

and the tr-component of the Einstein equations is:

$$\frac{R_{,r}}{R}\frac{\dot Q}{Q} = -\kappa\dot\phi\phi_{,r}. \qquad (3)$$

The rr-component of Eq. (1) reads:

$$\left(R_{,t}^2 R + kR \right)_{,t} + Q_{,t}R = \qquad (4)$$

$$-\kappa\left(\frac{1}{2}\dot\phi^2 + \frac{Q}{2R_{,r}^2}\phi_{,r}^2 - V(\phi) \right) R_{,t}R^2.$$

¿From $T^{(m)\,a}{}_{b;a} = 0$, it follows that:

$$\kappa\varepsilon^{(m)} = \frac{F(r)\sqrt{Q(r,t)}}{R_{,r}R^2}, \qquad (5)$$

where $F(r)$ is an arbitrary constant of integration. If we define r so that $R(r,t_i) = r$ for some $t = t_i$, then $F(r) = 2M_{i,r}(r)/\sqrt{Q(r,t_i)}$ where $M_i(r)$ is the mass inside a shell of radius r at $t = t_i$.

¿From $T^{(\phi)\,a}{}_{b;a} = 0$ one obtains:

$$-\Box\phi = V_{,\phi}(\phi). \qquad (6)$$

Eq. (6) is subject to the boundary conditions: $\phi_{,r} = 0$ at $R = 0$, and $\phi_c(t) = \lim_{r\to\infty}\phi(r,t)$, where $\phi_c(t)$ is the solution of Eq. (6) in the cosmological background. We make the following definitions:

$$2M(r,t) = \int_{r_0(t)}^{r} F(r)\sqrt{Q(r,t)}\,\mathrm{d}r,$$

$$\varepsilon_c^{(\phi)} = \frac{1}{2}\dot\phi_c^2 + V(\phi_c),$$

$$\delta\varepsilon^{(\phi)} = \frac{1}{2}\dot\phi^2 + \frac{Q}{2R_{,r}^2}\phi_{,r}^2 + V(\phi) - \varepsilon_c(t),$$

$$\delta\tilde\varepsilon^{(\phi)} = \delta\varepsilon^{(\phi)} - R_{,t}\dot\phi\frac{\phi_{,r}}{R_{,r}},$$

where $r_0(t)$ is defined by $R(r_0(t), t) = 0$. We also define:

$$P_c^{(\phi)}(t) = \frac{1}{2}\dot{\phi}_c(t) - V(\phi_c),$$

$$\delta P^{(\phi)}(r, t) = \frac{1}{2}\dot{\phi}^2 + \frac{Q}{2R_{;r}^2}\phi_{,r}^2 - V(\phi) - P_c^{(\phi)}(t).$$

Integrating Eqs. (3) and (5) and using Eqs. (3) and (6) we find that

$$R_{,t}^2 = -k(r, t) + \frac{2M(r, t)}{R} + \frac{1}{3}R^2\kappa\varepsilon_c^{(\phi)}(t)$$

$$+ \frac{\kappa}{R}\int_{r_0(t)}^{r} R_{,r}(z, t)R^2(z, t)\,\delta\tilde{\varepsilon}^{(\phi)}(z, t)\,\mathrm{d}z, \quad (7)$$

and

$$R_{,tt} = -\frac{M(r, t)}{R^2} - \frac{1}{6}R\left(\kappa\varepsilon_c^{(\phi)} + 3\kappa P_c^{(\phi)}\right) - \quad (8)$$

$$\left[\frac{\kappa}{2R^2}\int_{r_0(t)}^{r} R_{,r}(z, t)R^2(z, t)\,\delta\tilde{\varepsilon}^{(\phi)}(z, t)\,\mathrm{d}z + \frac{1}{2}R\kappa\delta P^{(\phi)}\right]$$

As $R \to \infty$ we must recover the FRW background cosmology which implies:

$$\lim_{r \to \infty} M(r, t) \sim \frac{1}{2}\kappa\varepsilon_c^{(m)}(t_0)a^3(t_0)r^3,$$

$$\lim_{r \to \infty} k(r, t) \sim k_0 r^2,$$

where t_0 is an arbitrary time, $a(t)$ is the scale factor of the FRW background, and k_0 is the curvature of the background. In line with current observations, and because it greatly simplifies the calculations, we take the cosmological background to be flat and set $k_0 = 0$. We do not attempt to solve the Einstein or DDE equations exactly, but instead we develop asymptotic approximations to the true solutions which are accurate so long as a number of parameters, which we define and interpret below, remain small.

3. SMALL PARAMETERS AND THE MATCHED ASYMPTOTIC EXPANSIONS.

One can think of the small parameters approach and the matched asymptotic expansions as an expansion in the Newtonian potential. Although it is perhaps fairer to say that is closest to the context of General Relativity. The differences are not obvious at leading order but at next to leading order one will see that what appears in the equation for the acceleration is not necessarily what one would expect to appear in the Non-relativistic regime.

As stated above in Section 2.1, we require that gravity is 'suitably weak' inside the density perturbation. By suitably weak we mean that

$$|\delta_1| \ll 1,$$

where

$$\delta_1 = \delta v \equiv R_{,t} - HR.$$

Physically $R_{,t}$ is the velocity of a particle of dust in $\{t, R\}$ coordinates, where R is the physical radial coordinate, and HR is the velocity that such a particle would have in the cosmological background. The small parameter $\delta_1 = \delta v$ is therefore the peculiar velocity of a matter particle with respect to the cosmological background. Recall that
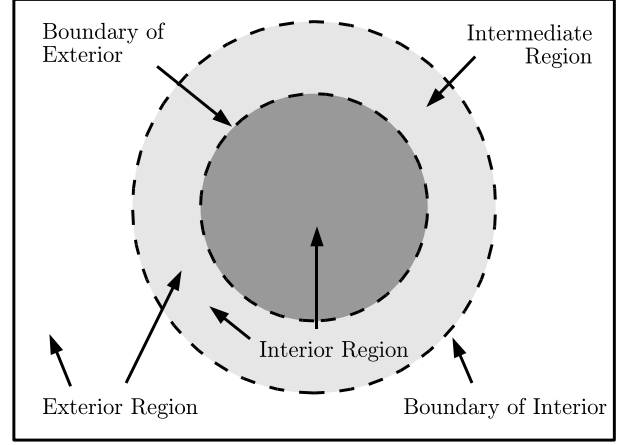

FIG. 1.— Sketch showing the interior, exterior and intermediate regions. The interior is defined to be the region where the inner approximation is valid, and the exterior is the region where the outer approximation is applicable. In order for the matching procedure to work, we must require that the exterior and interior regions overlap in some intermediate region. We must also require the exterior and interior regions are contiguous, so that one may move smoothly from the exterior, through the intermediate region, to the interior.

we use units where $c = 1$, hence the first expression above is in fact the dimensionless quantity $\delta v/c \ll 1$. Our assumption requires that whenever $HR \gtrsim \mathcal{O}(1)$, we have $|\delta_1/HR| \ll 1$. This condition is equivalent to requiring that the mean matter density contrast, $\bar{\delta}(R, t)$, inside the sphere with radius $R \sim \mathcal{O}(1/H)$ or greater, is small enough that it may be treated as a linear perturbation about the cosmological background. The mean matter perturbation is however allowed to be non-linear, $\bar{\delta} \gtrsim \mathcal{O}(1)$, when $HR \ll 1$ provided $|R_{,t}| \ll 1$. We also define

$$\delta_2 = \frac{1}{3}R^2\kappa(\varepsilon^{(m)} - \varepsilon_c^{(m)}) \equiv \frac{1}{3}R^2\varepsilon_c^{(m)}\delta_m.$$

We require $\delta_2 \ll 1$. This again require that $\delta_m \gtrsim 1$ only when $HR \ll 1$ i.e. the matter perturbation is only non-linear on sub-horizon scales. We note that $\delta_2 \sim \mathcal{O}((R_{,t}^2 + k) - H^2R^2)$, and so generally $|\delta_1| \ll 1$ provided $\delta_2 \ll 1$.

In what follows we assume that δ_1 and δ_2 are small *everywhere*. These assumptions can be checked once one specifies initial conditions for the matter overdensity, but they generally hold very well whenever the scale of the inhomogeneous region is $< 0.1/H$.

We now define two over-lapping regions which we shall refer to as the interior and the exterior.

3.1. *The Interior Region*

The *interior region* is defined by

$$\delta_3 \equiv HR \ll 1.$$

We define the *inner limit* of a quantity $F(r, t)$ to be $L_{int}(F) = \lim_{\delta_3 \to 0} F(r, t)$. The inner limit can be imagined as the limit in which the cosmological background density of matter is taken to zero, and the cosmological horizon is taken to infinity. In the interior we construct asymptotic approximations to quantities in the limit $HR \to 0$. We also expand in δ_1 and δ_2. We refer to this as the *inner approximation*.

3.2. *The Exterior Region*

In the *exterior region*, spacetime is required to be homogeneous and isotropic at leading order. In other words, the matter perturbation must be linear in the exterior:

$$\delta_4 \equiv |\delta_1/\delta_3| \ll 1, \delta_5 = |\delta_m| \ll 1.$$

From the form of $R_{,t}$, it is clear that $\delta_5 \to 0$ implies $\delta_4 \to 0$. We define the *exterior limit* of a quantity $F(r,t)$ to be $L_{ext}(F) = \lim_{\delta_5 \to 0} F(r,t)$. As in the interior limit we also expand in δ_1 and δ_2. We construct asymptotic approximations to quantities in the exterior region in this exterior limit and refer to them as the *outer approximations*.

3.3. *Matching and the Intermediate Region*

We are primarily concerned with the behaviour of the DDE in the interior region. In Section 4, we find the inner approximation to ϕ by solving Eq. (6) order by order in the interior limit. We cannot, however, apply both of the boundary conditions on ϕ directly to the inner approximation. This is because the condition $\lim_{R \to \infty} \phi = \phi_c(t)$ must be applied at $R = \infty$, a point that is very clearly in the exterior and *not* in the interior region. As a result, the inner approximation will contain ambiguous constants of integration. Fortunately, this ambiguity can be lifted by matching the inner and outer approximations to ϕ if there exists some *intermediate region* where both approximations are simultaneously valid. This matching of the inner approximation to the outer one is referred to as the method of matched asymptotic expansions (MAEs). It relies on the fact that, in any given region, the asymptotic expansion of a quantity is unique (for a proof see Hinch 1991). Thus if the inner and outer approximations of ϕ are both valid in the intermediate region, they must be equal in that region. For the method of MAE to be applicable we must, of course, require that an intermediate region exists. A necessary condition for an intermediate region to exist is that for some range of R:

$$HR \ll 1, \quad |3\delta_2/\kappa\varepsilon_c^{(m)}(t)R^2| = |3\delta_m(t)/\kappa| = \ll 1.$$

This becomes a necessary and sufficient condition if the only boundary of the interior region is in the exterior one, and vice versa (see Figure 1 for an illustration). If the scale of the inhomogeneity, R_0, is taken to be the largest value of R for which $|3\delta_2/\kappa\varepsilon_c^{(m)}(t)R^2| > 0.3$, and then then an intermediate region generally exists provided that $R_0 \lesssim 0.1H$.

In resume, in this section we have considered spherically symmetric backgrounds and far from black hole horizons. We have basically performed an expansion in the Newtonian potential at leading order, at least as far as the evolution of scalar field perturbations are concerned. Notice, however, that this method can be straightforwardly extended to allow for deviations from spherical symmetry (Shaw & Barrow 2006a,b,c).

To be clear, we should point out that the expansion in δ_1 and δ_2, which is a lot like expanding in the Newtonian potential, is not really the key to our method. That is just a simplification. The key is that we take: $\delta_3 = HR \ll 1$ in the interior region and $\delta_m \ll 1$ in the exterior region. That is, everything is linear in those

two regions. We then assume that there is an intermediate region where both of these conditions hold. Which implies that in the intermediate region: $|\delta_1| \ll 1$ and $|\delta_2| \ll 1$. So the assumption that $\delta_1, \delta_2 \ll 1$ everywhere ensures that we have an intermediate region. We could in fact relax this but the calculations would become more difficult: often still doable, but in almost all physically interesting cases totally unnecessary. For instance the relaxation to $|\delta_1| < 1$ and $|\delta_2| \ll 1$, is very straightforward and allows one to go all the way up to a black hole horizon (Shaw & Barrow 2006a,b,c).

4. EVOLUTION OF DYNAMICAL DARK ENERGY PERTURBATIONS

In this section we find an asymptotic approximation to the DDE density contrast, δ_ϕ. The discussion is fairly technical, and readers more interested in the results than the machinery used to derive them may prefer to focus on the statement, discussion and application of our results in Section 4.3 and following.

The DDE is described by the field ϕ which satisfies:

$$-\Box\phi = V_{,\phi}(\phi).$$

We solve this equation by constructing an asymptotic approximation to ϕ in the small parameter δ_1. We write:

$$\phi \sim \phi_c(t) + \delta\phi(t,r)(1 + \mathcal{O}(\delta_1)),$$

where $\delta\phi \sim \mathcal{O}(\delta_1)$. Before solving for ϕ, we make the dependence of the metric on δ_1 explicit by transforming to a new radial coordinate, $\rho = R(t,r)/a(t)$, where $a(t)$ is the scale factor of the Friedmann-Robertson-Walker (FRW) cosmological background. In $\{t, \rho\}$ coordinates the metric is:

$$ds^2 = \frac{(1 - k(r,t) - \delta_1^2(r,t))\,dt^2}{1 - k(r,t)} + 2\frac{\delta_1(r,t)a(t)\,dt\,d\rho}{1 - k(r,t)} -$$
$$\frac{a^2(t)\,d\rho^2}{1 - k(r,t)} - a^2\rho^2\left\{ d\theta^2 + \sin^2\theta\,d\varphi \right\}. \qquad (9)$$

Consider $-\Box\phi_c(t)$ in this metric:

$$-\Box\phi_c(t) = V_{,\phi}(\phi_c) + \frac{1}{2}\frac{\dot{Q}}{Q}\dot{\phi}_c(t) - \frac{\dot{\phi}_c(t)}{a(t)\rho^2}\frac{\partial}{\partial\rho}\left(\rho^2\delta_1\right).$$

where $\dot{Q}$ is evaluated at constant r as opposed to constant ρ or R and is thus given by Eq. (3). It follows that $\delta\phi$ satisfies:

$$-\Box\,\delta\phi\,(1 + \mathcal{O}(\delta_1)) = (V_{,\phi}(\phi) - V_{,\phi}(\phi_c)) \qquad (10)$$
$$+ \frac{1}{2}\kappa\dot{\phi}_c^2(t)\rho\delta\phi_{,\rho} + \frac{\dot{\phi}_c(t)}{a(t)\rho^2}\left(\rho^2\delta_1\right)_{,\rho}.$$

We now solve for $\delta\phi$ in both the interior and exterior regions.

4.1. *Inner Approximation*

We note that $\frac{1}{2}\kappa\dot{\phi}_c^2 R^2 \lesssim \mathcal{O}(\delta_3^2)$, and that $|k| \sim \mathcal{O}(\delta_3, \delta_1^2, \delta_2)$, so that

$$-\frac{\rho^2}{a}\partial_t\left(a^3(t)\delta\phi_{,t}\right) + \left(\rho^2\delta\phi_{,\rho}\right)_{,\rho} \sim (V_{,\phi}(\phi) - V_{,\phi}(\phi_c))\,a^2\rho^2$$
$$+ \dot{\phi}_c(t)a\left(\rho^2\delta_1\right)_{,\rho} + \mathcal{O}(\delta_1\delta\phi, \delta_2\delta\phi, \delta_3^2\delta\phi).$$

In many cases $\delta\phi$ is small enough so that

$$(V_{,\phi}(\phi) - V_{,\phi}(\phi_c))a^2\rho^2 \sim V_{,\phi\phi}(\phi_c)R^2\delta\phi,$$

6

and $V_{,\phi\phi} \sim \mathcal{O}(H^2)$ so that $\phi_c(t)$ evolves over cosmological time-scales. In these cases it is clear that:

$$(V_{,\phi}(\phi) - V_{,\phi}(\phi_c))a^2\rho^2 \sim \mathcal{O}(\delta_3^2 \delta\phi),$$

and so this term can be dropped at leading order. Although it will often be the case that $V_{,\phi}(\phi) - V_{,\phi}(\phi_c) \approx V_{,\phi\phi}(\phi_c)\delta\phi$ we do not have to require such a strong assumption in order to justify ignoring the effect of the potential to leading order in the interior approximation. Instead, we make the far weaker assumption that:

$$|V_{,\phi}(\phi_c + \delta\phi) - V_{,\phi}(\phi_c)|R^2/\delta\phi \sim \mathcal{O}(\delta_1, \delta_2, \delta_3). \quad (11)$$

A physically-viable DDE theory for which this requirement does not hold would be difficult to construct. For instance, if this condition did not hold then even if, at one instant, $V_{,\phi}(\phi_c) \sim \mathcal{O}(H^2)$ or smaller, as must be required for ϕ_c to evolve over cosmological time scales, shortly afterwards small changes in ϕ_c would cause $V_{,\phi}(\phi_c)$ to grow to be many orders of magnitude greater than H^2. This would result in ϕ_c evolving over time-scales that are much shorter than the Hubble time. The only DDE theories that we can imagine that could accommodate this and still be compatible with observations would involve ϕ being held almost completely fixed at a minimum of $V(\phi_c)$, in which case the DDE would be almost entirely indistinguishable from a cosmological constant.

To leading order in the interior, we would actually be justified in setting $a(t) = \text{const}$ as $\dot{a}\rho = HR = \delta_1 \ll 1$. However, since it might not be completely clear that these terms may be ignored, and because we can solve the $\delta\phi$ equation without having to ignore them, we continue to include them.

We define $d\eta = dt/a(t)$ and $u = a\delta\phi$, and note that $\rho^2 a_{,\eta\eta}/a = \dot{H}R^2 + H^2R^2 \sim \mathcal{O}(\delta_3)$, so that:

$$\left(-u_{,\eta\eta} + \frac{1}{\rho^2}\left(\rho^2 u_{,\rho}\right)_{,\rho}\right)(1 + \mathcal{O}(\delta_1, \delta_2, \delta_3)) \sim$$
$$\dot{\phi}_c(t)\frac{1}{\rho^2}\left(a(t)\rho^2\delta_1\right)_{,\rho}. \quad (12)$$

which has as a solution

$$\delta\phi(t,\rho) \sim -\frac{1}{2}\int_0^\infty \rho'^2\, d\rho' \int_{-1}^1 ds\, \frac{f(\eta(t) - X, \rho')}{a(t)X(\rho, \rho', s)} +$$
$$\frac{\mathcal{F}(\eta - \rho)}{a(t)\rho} + \frac{\mathcal{G}(\eta + \rho)}{a(t)\rho} + \mathcal{O}(\delta_1\delta\phi, \delta_2\delta\phi, \delta_3\delta\phi), \quad (13)$$

where $f(\eta, \rho) = \frac{\dot{\phi}_c(t)a(t)}{\rho^2}\left(\rho^2\delta_1(t,\rho)\right)_{,\rho}$ and $X(\rho, \rho', s) = \sqrt{\rho^2 + \rho'^2 - 2\rho\rho's}$; $\mathcal{F}$ and $\mathcal{G}$ represent waves in the scalar field and we discuss them further momentarily. To go further, we make the following reasonable assumptions about the behaviour of δ_1. We assume that there exists some R_{-2}, in the interior region, such that for $R > R_{-2}$ in the interior region, δ_1 decreases faster than $1/R^2$ as $R \to \infty$; f then decreases faster than $1/R^3$ for $R > R_{-2}$. This assumption ensures that dominant contributions to the integral in Eq. (13) comes from values of ρ' that are well inside the interior region. Note that generally $f(\eta, \rho)$ varies over conformal times-scales of order $1/aH$ and $\delta_1/a\dot{\delta}_1$. Provided that δ_1 is not momentarily zero, these scales are much larger than $X \lesssim \sqrt{2}R_{-2}/a$ so we can Taylor expand $f(\eta - X, \rho')$ as

$$f(\eta - X, \rho') = f(\eta, \rho') + f_{,\eta}(\eta, \rho')X + \mathcal{O}(f_{,\eta\eta}X^2),$$

where the neglected terms are $\mathcal{O}(\delta_1^2, \delta_3^2, \delta_1\delta_3, \delta_2)$ times $f(\eta, \rho')$. After some algebra and integration we then arrive at:

$$\delta\phi(t,R)\left(1 + \mathcal{O}(\delta_1, \delta_2, \delta_3)\right) \sim \dot{\phi}_c(t)\int_\infty^R \delta_1(t, R')\, dR'$$
$$+ \frac{\mathcal{F}(\eta - \rho) + \mathcal{G}(\eta + \rho)}{R}. \quad (14)$$

where the previous assumption relating to the Taylor expansion of f can be seen to be equivalent to the statement that $\ddot{\delta}_1(t, R)R^2 \ll \delta_1$. This assumption will generally break down if there is some initial instant, $t = t_i$ say, when $\delta_1 = 0$. At $t \gg t_i$ however, $\ddot{\delta}_1 R^2 \ll \delta_1$ is equivalent to $\delta_1^2, \delta_3^2, \delta_2 \ll 1$, which is certainly the case in the interior region.

Generally, the functions $\mathcal{F}$ and $\mathcal{G}$ are related to the initial conditions on $\delta\phi$. Because we have required $R_{-2} \ll H^{-1}$ our analysis will break down at early times since generally $HR_{-2} \to \infty$ as $t \to 0$. As a result, we cannot generally determine $\mathcal{F}$ and $\mathcal{G}$ by simply specifying some initial conditions on$\delta\phi$, at $t = t_i$ say, and applying them to the interior approximation since the interior approximation by not be valid when $t = t_i$. The requirement that $\delta\phi(R = 0)$ can however be applied to the interior approximation to give $\mathcal{F}(\eta) = -\mathcal{G}(\eta)$. To the order at which we work, $\mathcal{F}(\eta)$ itself should be fixed by matching to the outer approximation.

4.2. Exterior Solution and Matching

In order for $\phi_c = \lim_{R\to\infty}\phi(t, R)$ we must have $\delta\phi(t, R) \to 0$ as $R \to \infty$. In the exterior region, space-time is FRW to leading order in δ_1 and δ_2, and the equation describing for the leading order behaviour of $u = a(t)\delta\phi$ reads:

$$-u_{,\eta\eta} + \frac{1}{\rho^2}\left(\rho^2 u_{,\rho}\right) = \left(V_{,\phi\phi}(\phi_c) - \dot{H} - H^2\right)a^2 u +$$
$$\frac{1}{2}\kappa\dot{\phi}_c^2(t)a^2\rho u_{,\rho} + \frac{\dot{\phi}_c(t)a^2}{\rho^2}\left(\rho^2\delta_1\right)_{,\rho}. \quad (15)$$

where $d\eta = dt/a(t)$. Solving this equation is far from straightforward. Fortunately, however, our main interest in not in how $\delta\phi$ behaves in the exterior region but in interior region where the perturbation in the matter density can be non-linear, and so it is not necessary to solve Eq. (15) in the exterior region so long as we know how its solutions behave in some intermediate region where $\delta_3 = HR \ll 1$. We require that $\delta\phi \to 0$ as the matter perturbation is removed i.e. $\delta_1 \to 0$. We have also required that δ_1 drop off faster than $1/R$ for $R > R_{-2}$ where R_{-2} is in the interior region i.e. $HR_{-2} \ll 1$. In this intermediate region, the solutions of Eq. (15) for which $\delta\phi \to 0$ as $R \to \infty$ have the following form:

$$\delta\phi(t, R) \sim \dot{\phi}_c(t)\int_{C(\eta)}^R \delta_1(t, R')\, dR' + \frac{K(\eta)}{R} +$$
$$\mathcal{O}(\delta_1\delta\phi, \delta_3\delta\phi, \delta_2\delta\phi), \quad (16)$$

where $C(\eta) \sim \mathcal{O}(1/H)$ or greater. We have assumed that t is larger compared to any initial instant when one one or more of $\delta_1 = 0$, $\delta\phi = 0$ or $\dot{\delta}\phi = 0$ hold. With these assumptions, matching to the interior region gives:

$$K(\eta) = \mathcal{F}(\eta) + \mathcal{G}(\eta) = 0,$$

and

$$\frac{2\mathcal{F}_{,\eta}(\eta)}{a(\eta)} = -\dot{\phi}_c(t)\int_C^\infty \delta_1(t, R')\, dR'.$$

We have required drop off of δ_1 means that, to leading order, we can set $C = \infty$. This implies that the $2\mathcal{F}_{,\eta}/a(\eta)$ is sub-leading order in the interior approximation and so may be neglected.

Thus to leading order in the interior region we find:

$$\delta\phi(t, R) \sim \dot{\phi}_c(t) \int_\infty^R \delta v(R', t)\, dR' \left(1 + \mathcal{O}(\delta_1, \delta_2, \delta_3)\right).$$

Where $\delta v = R_{,t} - HR$ is the peculiar radial velocity of the matter particles relative to the expansion of the background Universe. This approximation is valid in the interior region at late times compared to any initial instance when $\delta\phi = 0$ and/or $\delta\dot{\phi} = 0$ which is equivalent to $|\delta\ddot{v}|R^2 \ll |\delta\dot{v}|R \ll |\delta v|$. Note that, to this order, the surfaces of constant ϕ are surfaces of constant:

$$t_\phi = t - \int_R^\infty \delta v\, dR'.$$

We use this asymptotic approximation for $\delta\phi$ to evaluate the DDE density contrast on surfaces of constant t in the matter rest frame. In the rest frame of the matter particles:

$$\varepsilon^{(\phi)} = \frac{1}{2}\dot{\phi}^2 + \frac{Q}{2}\phi_{,R}^2 + V(\phi),$$

and the local inhomogeneity in $\varepsilon^{(\phi)}$ is therefore:

$$\delta\varepsilon^{(\phi)} \sim \dot{\phi}_c^2(t) \left(-3H \int_\infty^R \delta v(R', t)\, dR' + (\delta v(R, t))^2 \right.$$
$$\left. + \int_\infty^R \left(R_{,tt} - (\dot{H} + H^2)R' \right) dR' \right). \qquad (17)$$

The corrections terms are $\mathcal{O}(\delta_1, \delta_2, \delta_3)$ times smaller than the leading order term. Since $\dot{\phi}_c^2 = (1 + w)\varepsilon_c^{(\phi)}$ we have

$$\delta_\phi \sim (1 + w) \left(-3H \int_\infty^R \delta v(R', t)\, dR' + (\delta v(R, t))^2 \right.$$
$$\left. + \int_\infty^R \left(R_{,tt} - (\dot{H} + H^2)R' \right) dR' \right),$$

$R_{,tt}$ is the acceleration of the matter particles in (t, R) coordinates. Eq. (9) gives:

$$R_{,tt}R - \dot{H}R^2 - H^2R^2 \sim -\frac{\delta M}{R} + \mathcal{O}(\delta_3^3\delta_1,\ \delta_1^2\delta_3^2,\ \delta_2\delta_3^2).$$

where $\delta M(R, t) = M(R, t) - \frac{1}{2}\Omega_m H^2 R^3 = \frac{1}{2}\Omega_m H^2 R^3 \bar{\delta}$ is the mass contrast at time t inside the sphere with physical radius R.

4.3. Discussion

In this section we found that the DDE density contrast can be expressed, to leading order, in terms of the radial peculiar velocity, δv, the mean density contrast, $\bar{\delta}$ and the unperturbed DDE equation of state parameter w:

$$\delta_\phi \sim (1 + w) \left(3H \int_R^\infty \delta v(R', t)\, dR' + (\delta v)^2 \right.$$
$$\left. + \frac{1}{2}\Omega_m H^2 \int_R^\infty \bar{\delta}(R', t)R'\, dR' \right). \qquad (18)$$

This expression for δ_ϕ is our main result and it is valid for both linear and non-linear sub-horizon matter perturbations. In order to evaluate the above expression, one must simply specify the peculiar velocity, δv, of the matter particles and the matter density contrast $\bar{\delta}$. This exterior is valid in the interior region at late times compared to any initial instance when $\delta\phi = 0$ and/or $\delta\dot{\phi} = 0$ i.e. $|\delta\ddot{v}|R^2 \ll |\delta\dot{v}|R \ll |\delta v|$.

Note that H and w will depend on the mass of the field m, so in that sense, equation (18) is not completely model independent. However, all the model dependent terms come from the homogeneous and isotropic background cosmology. So the expression for δ_ϕ is model independent provided $mR_c \ll 1$. Which is true if $m \sim O(H)$ and $HR_c \ll 1$ as assumed.

The key point is that large deviations in δ_ϕ from the prediction using a LCDM background could only occur if δv and δ_m were predicted to change by an order of magnitude or more. As far as we know, however, structure formation is compatible with LCDM over the scales of clusters and so it seems unlikely that such large deviations occur.

As we shall see below the DDE perturbation is generally small compared to the matter perturbation, so to leading order one may neglect any DDE perturbations when evaluating $\bar{\delta}$ and δv.

It is interesting to note that the sign of δ_ϕ depends on the relative magnitudes of $\bar{\delta}$ and δv: From equation (18) one deduces that the formation of local overdensities or local voids of dark energy arise from two competing effects:

- The Drag effect: associated with deviations from $\delta v/HR = 0$. If one has an overdense region, then it expands more slowly. In agreement with Dutta & Maor (2007), we find this drag effect to produce a local underdensity of dark energy.

- The Pull effect: associated with deviations from $\delta_m = 0$. An overdensity of matter pulls the dark energy (and everything else) towards it. So matter and fields tend to clump around it. As a result, the pull effect means that an overdensity of matter creates an overdensity of DE.

So there is one effect that pulls the dark energy in and another that pushes it out. As we will see, in the linear regime the drag effect grows more quickly than the pull effect, so one gets a dark energy void. The onset of non-linear structure formation, however, causes $|\delta v/HR|$ to reach a maximum and then to tend to 1 at late times, whereas δ_m just keeps on growing. So the pull effect dominates at late times, so one ends up with an overdensity of dark energy.

We have assumed above that the mass of the DDE scalar field is small compared to the inverse length scale of the cluster. Provided this is δ_ϕ in uncoupled DDE theories is *independent* of the details of theory describing the dark energy.

In the next section we use Eq. (18) to evaluate δ_ϕ in both the linear and non-linear regimes. We find that $|\delta_\phi(R = 0)| \sim \mathcal{O}(\Omega_m H^2 R_c^2 \bar{\delta}_{clust})$, where R_c is the radial scale of the cluster, and $\bar{\delta}_{clust}$ is the mean matter density contrast in $R \le R_c$.

5. CLUSTERING OF DYNAMICAL DARK ENERGY

5.1. *Dynamical Dark Energy Clustering in the Linear Regime*

Although one of our main aim in this work was to study DDE clustering in the *non-linear* regime, our analysis is also perfectly valid in the linear regime, i.e. when $\delta_m \ll 1$, provided that the matter inhomogeneity is sub-horizon at the instant when we wish to evaluate δ_ϕ. We found above that δ_ϕ is given by Eq. (18). In the linear regime $|\delta v| \ll HR$, and so the term proportional δv^2 in Eq. (18) is small compared to the other two terms and should be neglected. $\delta_m(r,t)$ is the matter density contrast, and we define $\delta_k(t)$ to be its Fourier transform. In the linear regime (in comoving-coordinates):

$$\dot{\delta}_m = -\nabla \cdot \delta\mathbf{v},$$

and so:

$$\delta v_k = -\frac{iHf(a)a\delta_k}{k},$$

where $f(a) = \mathrm{d}\ln\delta_k/\mathrm{d}\ln a$ and δv_k is the Fourier transform of δv. We recognize that $3\Omega_m H^2 \bar\delta R/2 = \delta M/R^2 = \partial\delta\Phi/\partial R$ where $\delta\Phi$ is the leading order perturbation to the Newtonian potential. $\delta\Phi$ is given by:

$$\nabla^2\delta\Phi = 4\pi G\delta_m.$$

The Fourier transform of $\bar{\delta}(R,t)R$ is therefore: $ia\delta_k/k$, and the Fourier transform of the DDE density contrast, δ_ϕ, in the linear regime is given by:

$$\delta_{\phi k}^{(\mathrm{lin})} \sim -\frac{3}{2}(1+w)g(a)\frac{a^2\Omega_m H^2\delta_k}{k^2}. \qquad (19)$$

where

$$g(a) = \frac{2f(a)}{\Omega_m} - 1. \qquad (20)$$

Motivated by observations, we assume $(1+w)$ to be small at late times, and $(1-\Omega_m)$ to be small at early times. To a first approximation then we approximate $f(a)$ by its ΛCDM value. At late times a very good approximation to $f(a)$ in the ΛCDM model is $\Omega_m^{0.6}$ (Peebles 1980; Lahav et al. 1991). Note that corrections to this fitting formulae occur for quintessence-like models (Wang & Steinhardt 1998). However, these are generally too small to greatly affect our results. Hence we take the ΛCDM expression for simplicity. Even when it is not acceptable to approximate $f(a)$ by its ΛCDM, we do not expect this approximation to greatly alter the qualitative nature of our results or the order of magnitude of δ_ϕ.

Transforming back into real space we have:

$$\delta_\phi^{(\mathrm{lin})} \sim -\frac{(1+w)g(a)\Omega_m a^2 H^2}{2}\int_r^\infty r'\bar{\delta}(r',t)\,\mathrm{d}r', \quad (21)$$

Our expression for $\delta_{\phi k}^{(\mathrm{lin})}$ is independent of the mass of ϕ. This is because we have assumed that $m_\phi \sim \mathcal{O}(H)$ in the linear regime and that the matter perturbation is small compared with H^{-1}. The mass of the scalar field therefore has only a negligible effect on the scales over DDE clustering occurs. It is clear that the sign of $\delta_{\phi k}$ is the same as the sign of $-g(a)\delta_k$. At late times $g(a) > 0$, and so a linear local overdensity of matter ($0 < \delta_m \ll 1$) corresponds to a DDE void. Similarly, there is a DDE overdensity at late times (in the linear

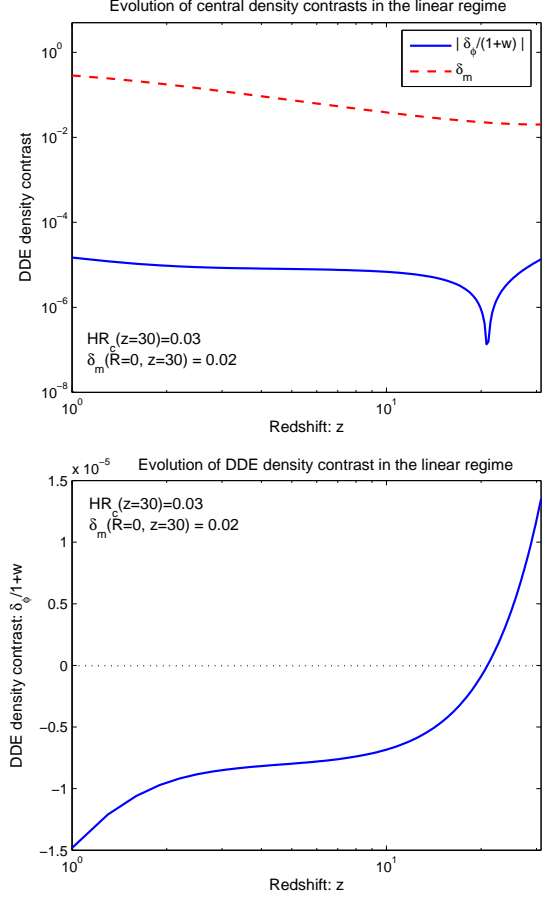Evolution of central density contrasts in the linear regime

FIG. 2.— Evolution of the DDE and matter density contrasts in the linear regime for an overdensity that begins to collapse at $z = z_i = 30$. We have taken $\Omega_m(z = 0) = 0.27$. Initially the matter density profile is taken to be Gaussian with $\delta_m(z_i, r = 0) = 0.02$ and $H_i r_c = 0.03$. This corresponds $\delta_m(r = 0) = 0.3$ and $R_c = ar_c \approx 31h^{-1}$Mpc today. $|\delta_\phi|$ is always small compared to δ_m. At early times, the DDE density contrast is positive however it must be noted that our approximation is only valid in this case for $z \lesssim 29$. At late times it is negative. We can see that $|\delta_\phi/(1+w)|$ is growing at late times in the linear regime; indeed it is in fact growing faster than δ_m for $z < 0.23$.

regime) if there is a local void of matter. If an initial mean density perturbation $\delta_k(z_i)$ begins to collapse at $z = z_i$ when $a = a_i = 1$, $\Omega_m = \Omega_{mi}$ and H_i we have:

$$\delta_k \approx \frac{1}{3\Omega_{mi}^{0.4} + 2} \qquad (22)$$
$$\left(3\Omega_{mi}^{0.4}\left(\frac{\Omega_m}{\Omega_{mi}}\right)^{0.2}a + 2\left(\frac{\Omega_{mi}}{\Omega_m}\right)^{0.5}a^{-3/2}\right)\delta_k(z_i),$$

and so

$$\delta_{\phi k}^{(\mathrm{lin})} \sim \frac{9(1+w)\Omega_{mi}H_i^2}{6\Omega_{mi}^{0.4} + 4}\left(\Omega_{mi}^{0.4}(2\Omega_m^{-0.4} - 1)\left(\frac{\Omega_m}{\Omega_{mi}}\right)^{0.2}\right.$$
$$\left.-\frac{8}{3}\left(\frac{\Omega_{mi}}{\Omega_m}\right)^{0.5}\left(\frac{1+z}{1+z_i}\right)^{5/2}\right)\frac{\delta_k(z_i)}{k^2}.$$

Our expression for δ_ϕ was derived under the assumption that $|\delta\ddot{v}|R^2 \ll |\delta\dot{v}|R \ll |\delta v|$. As result it will break

down as we approach $z = z_i$. More precisely, we find that our approximation is valid at $R = 0$ for $a \gtrsim a_i(1 + 2H_iR_{-2}(z_i))$ i.e. $z \lesssim z_{app} \equiv z_i(1 - 2H_iR_{-2}(z_i))$ where H_i is the initial value of H and $R_{-2}(z_i)$ is the initial value of R_{-2}. ¿From this expression we can see that a matter *overdensity* corresponds initially to a DDE *overdensity* ($\delta_\phi^{(\mathrm{lin})} > 0$), however this DDE overdensity becomes a DDE void at some $z = z_{crit}$, and $\delta_\phi^{(\mathrm{lin})} < 0$ for $z < z_{\mathrm{crit}}$. We see that z_{crit} is given by:

$$\frac{1 + z_{\mathrm{crit}}}{1 + z_i} \approx \Omega_m^{-0.6}(z_{\mathrm{crit}}) \left(\frac{6 - 3\Omega_m^{0.4}(z_{\mathrm{crit}})}{8} \right)^{2/5},$$

where we have taken $\Omega_{mi} \approx 1$. If $\Omega_m(z_{\mathrm{crit}}) = 1$, which should be a good approximation for $1.8 \lesssim z \lesssim 3000$, we have $z_{\mathrm{crit}} = (3/8)^{2/5}(1 + z_i) - 1$. For this analysis to be valid we must have $z_{\mathrm{crit}} < z_{app}$ which with $\Omega_m(z_{\mathrm{crit}}) \approx 1$ holds $H_iR_{-2}(z_i) \lesssim 0.24$. For inhomogeneities that are larger than this at $z = z_i$ we do *not* expect z_{crit} to be an accurate approximation to the redshift when the DDE density contrast changes sign.

Note that z_{crit} does not depend on the size of the inhomogeneity, although, of course, we must have $z_{\mathrm{crit}} \lesssim z_{app}$ for our analysis to be valid, which implies that at $z = z_{\mathrm{crit}}$, $HR_{-2} \lesssim 0.2$.

If $\Omega_m = 1$ exactly then $\delta_\phi^{(\mathrm{lin})}/(1 + w) \to$ const at late times. If $\Omega_m < 1$, then $|\delta_\phi/(1 + w)|$ grows likes:

$$\left| \frac{\delta_\phi}{1 + w} \right| \propto 2\Omega_m^{-0.2} - \Omega_m^{0.2},$$

at late times in the linear regime. This implies that $|\delta_\phi/(1 + w)|$ tends to a constant in the linear regime if $\Omega_m = 1$, and is growing for $\Omega_m < 1$. At late times in the linear regime then: $|\delta_\phi/\delta_m| \propto \Omega_m^{-0.4}a^{-1}$. If we take $\Omega_m = 0.27$ today then $|\delta_\phi^{(\mathrm{lin})}/(1 + w)|$ is predicted to grow faster than δ_m when $z = 0.23$. Dutta & Maor (2007) also found that at late times in the linear regime $|\delta_\phi/(1+w)|$ grows faster than δ_m. This is behaviour were to continue into the non-linear regime it would, of course, imply that $|\delta_\phi/(1 + w)|$ would ultimately grow to be very large and indeed dominate over δ_m. As we show in this paper, however, before this can happen the matter perturbation goes non-linear and this slows the growth of $|\delta/(1 + w)|$.

We conclude our analysis of the linear regime by noting that Eq. (21) implies that at late times:

$$\delta_\phi^{(\mathrm{lin})}(r = 0, t) \approx \qquad (23)$$
$$-\frac{3C_\delta(1 + w)}{2}(2\Omega_m^{0.6} - \Omega_m)H^2(ar_{-2})^2\bar{\delta}(r_{-2}, t),$$

where r_{-2} is defined the smallest value of r for which $\partial \ln \bar{\delta}/\partial \ln r \geq -2$, and $C_\delta \sim \mathcal{O}(1)$ depends on the precise form of $\bar{\delta}$.

We have shown that in the linear regime $|\delta_\phi|$ at the centre of the inhomogeneity is always smaller than $|\bar{\delta}(r_{-2}, t)|$ by a factor of about $(1 + w)(Har_{-2})^2$; Har_{-2} is roughly equal to the physical size of the inhomogeneity as a fraction of the horizon size. If the initial density perturbation is Gaussian i.e.

$$\delta_m(z_i) = \delta_0 \exp(-r^2/r_c^2)$$

then

$$\delta_i(r) = \frac{3\delta_0 r_c^3}{4r^3}\sqrt{\pi}\mathrm{erf}(\frac{r}{r_c}) - 2\frac{r}{r_c}e^{-(r/r_c)^2}$$

and:

$$\delta_\phi^{(lin)}(r = 0, t) \approx -\frac{9(1 + w)\delta_0 H_i^2 r_c^2}{20}(2\Omega_m^{-0.2} - \Omega_m^{0.2}),$$

at late times.

We plot the evolution of $\delta_m(r = 0)$ and $\delta_\phi(r = 0)$ for a Gaussian initial matter density perturbation in the linear regime in Figure 2. We have assumed that $\delta_m(r = 0, z_i) = 0.02$ at $z_i = 30$, and $H_i r_c = 0.03$, which corresponds to and $\delta_m(r = 0, z = 0) = 0.3$ and $Har_c = 0.010$ today i.e. $R_c = ar_c \approx 31h^{-1}$ Mpc. For this choice of inhomogeneity, our approximation for δ_ϕ is only good for $1 + z \lesssim 0.94(1 + z_i) \approx 29$. Just as Dutta & Maor (2007) saw in their numerical simulations, we find that close to $z = z_i$, $\delta_\phi/(1 + w) > 0$. It then becomes negative, and at late times it continues to grow more negative, and it appears as if it might overtake δ_m at some point in the future. However, as we shall show below, this does not occur and $|\delta_\phi|$ remains small at all times. Note that the apparent increase in δ_ϕ at early times is due in part to fact that our approximation breaks down as one approaches $z = z_i$. If one wishes to study the evolution of δ_ϕ all the way back to $z = z_i$, the numerical approach taken by Dutta & Maor (2007) provides accurate results. Our real focus in this work is, however, not on what occurs at very early times in the linear regime, but how the DDE density contrast evolves when the matter inhomogeneity goes non-linear. We consider this below.

5.2. *Dynamical Dark Energy Clustering in the Quasi-Linear Regime*

We begin our investigation of how δ_ϕ evolves when the matter perturbation exits the linear regime by considering a matter perturbation that is in the weakly non-linear or quasi-linear regime i.e. $-1 < \bar{\delta} \lesssim 10$. Eqs.(3) and (5) give $M(r, t)/R \sim M(r)/R + \mathcal{O}(\delta_3^3\delta_1, \delta_1^2\delta_3^2, \delta_2\delta_3^2)$. We suppose that at some initial time, t_i, $R_{,t} = HR$ and $R = r$. $M(r)$ is then the mass inside the shell with radius r at $t = t_i$. We write:

$$M(r) = \frac{\Omega_m(t_i)}{2}H_i^2 r^3(1 + \delta_i(r)).$$

$\delta_i(r)$ is interpreted as the initial mean matter density contrast. In the full non-linear regime, which we consider in the next subsection, we are only able to evaluate $R(r, t)$ and hence, via Eq. (18), δ_ϕ, analytically in a matter-dominated background ($\Omega_m = 1$). In many cases of interest, however, $\delta_m \sim \mathcal{O}(1)$, e.g. superclusters and voids. Although the linear approximation fails for such objects, a good leading approximation to the true mean density contrast of matter, $\bar{\delta}$, in the range, $-1 < \bar{\delta} \lesssim 10$ is given by:

$$1 + \bar{\delta}(r, t) \approx \left(1 - 2\bar{\delta}_{\mathrm{lin}}(r, t)/3 \right)^{-3/2},$$

where $\bar{\delta}_{\mathrm{lin}}$ is the linear mean density contrast. This approximation improves as $\Omega_m \to 0$ and is exact for $\Omega_m = 0$. When this approximation holds we say that we are in the quasi-linear regime.

Evolution of central density contrasts for a typical supercluster

Evolution of central density contrasts for a typical void

Evolution of DDE density contrast for a typical supercluster

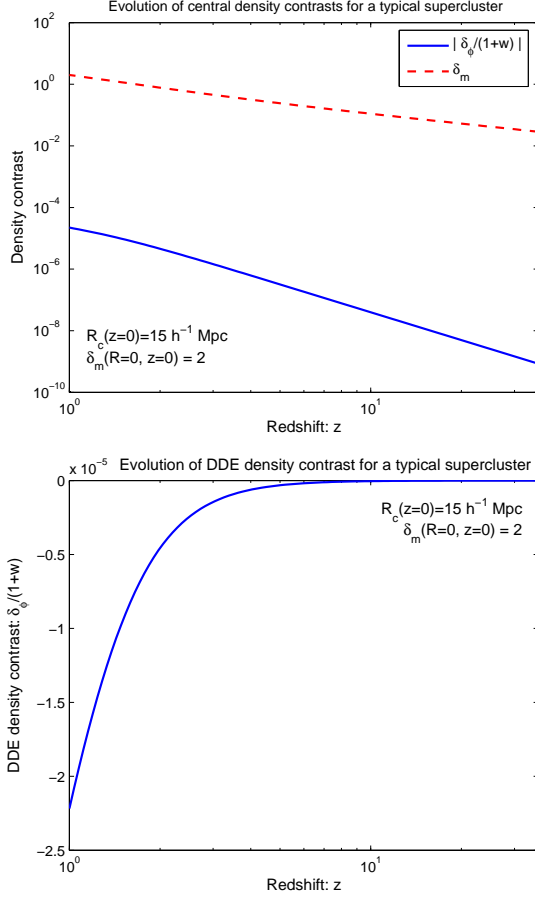Evolution of DDE density contrast for a typical void

FIG. 3.— Evolution of the DDE and matter density contrasts for a supercluster which today has a core matter overdensity of 2 and a core radius of $15h^{-1}$ Mpc. We have take $\Omega_m = 0.27$ today. $|\delta_\phi|$ is always $\ll \delta_m$, and $\delta_\phi/(1+w) < 0$ which corresponds to a DDE void. As in the linear regime, $|\delta_\phi/(1+w)|$ grows monotonically with time, and at late times $|\delta_\phi/(1+w)|$ is growing more quickly than δ_m.
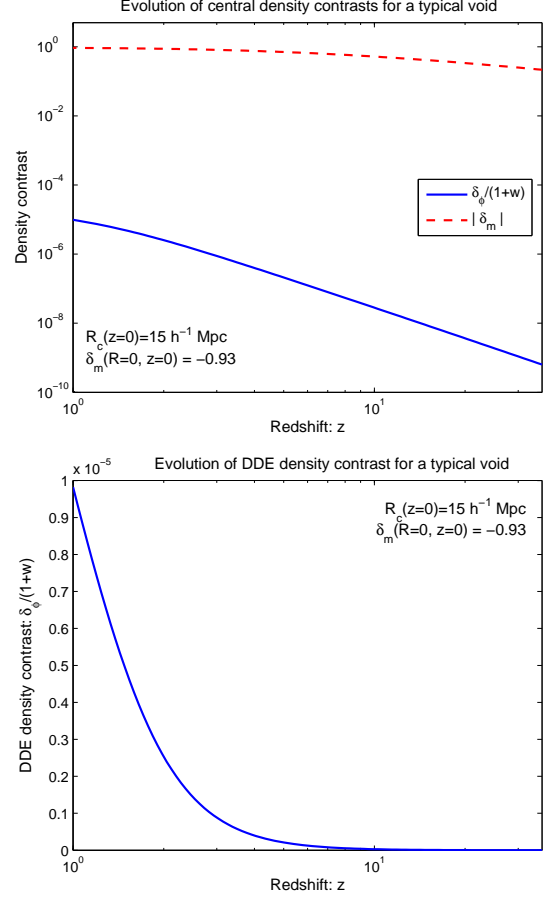
FIG. 4.— Evolution of the DDE and matter density contrasts for a typical void which today has a core matter density contrast of -0.93 and a core radius of $15h^{-1}$ Mpc. We have taken $\Omega_m = 0.27$ today. $|\delta_\phi|$ is always $\ll |\delta_m|$, and $\delta_\phi/(1+w) > 0$ which corresponds to a DDE overdensity. As in the linear regime, $|\delta_\phi/(1+w)|$ grows monotonically with time and at late times $|\delta_\phi/(1+w)|$ is growing more quickly than $|\delta_m|$.

In this section we find $\delta_\phi(\bar{\delta})$ for inhomogeneities in the quasi-linear regime. We are again assuming that any deviations from the ΛCDM model for structure formation due the background DDE evolution are sub-leading order i.e. $(1 - \Omega_m)(1 + w)$ is small. If this is not the case then our expression for δ_ϕ in terms of $\bar{\delta}$ and δv is still valid, but the evolution of $\bar{\delta}$ and δv would change; even still the order of magnitude of δ_ϕ would not be greatly effected.

The peculiar velocity, $\delta v = R_{,t} - HR$, is related to $\bar{\delta}(r, t)$ thus:

$$\delta v = -\frac{\bar{\delta}_{,t} R}{3(1 + \bar{\delta})} \approx -\frac{1}{2} HRf(a)((1 + \bar{\delta})^{2/3} - 1),$$

where, as above, $f(a) \approx \Omega_m^{0.6}$ at late times. In the quasi-linear regime the *physical radius*, $R(r, t)$, of a shell with mass $M(r)$ is given by:

$$R = a \left(1 - \frac{2\delta_{\text{lin}}(r, t)}{3}\right)^{1/2} \left(\frac{2M(r)}{a_i^3 \Omega_{m\,i} H_i^2}\right)^{1/3}$$

$$= ar \left(1 - \frac{2\delta_{\text{lin}}(r, t)}{3}\right)^{1/2} (1 + \delta_i(r))^{1/3}. \quad (24)$$

Using Eq. (18), we find that the dark energy density contrast, δ_ϕ, in the quasi-linear regime is well approximated by $\delta_\phi^{(\text{ql})}$ where:

$$\delta_\phi^{(\text{ql})} \equiv \quad (25)$$

$$-\frac{(1+w)\Omega_m H^2}{2} \int_R^\infty dR'\, R' \left(\frac{3f(a)((1+\bar{\delta})^{2/3} - 1)}{\Omega_m} - \bar{\delta}\right)$$

$$+\frac{(1+w)\Omega_m H^2 R^2}{4} \left(\frac{f(a)^2}{\Omega_m}\right)((1+\bar{\delta})^{2/3} - 1)^2.$$

For $0.27 \leq \Omega_m \leq 1$, the first term in Eq. (25) is negative definite for all positive values of $\bar{\delta}$ for which the quasi-linear approximation holds ($0 < \bar{\delta} \lesssim 10$) and positive definite for $-1 < \bar{\delta} < 0$. The second term in Eq. (25) is clearly positive definite but vanishes at $R = 0$. The relative magnitude of the two terms depends on the choice of initial density profile. However, at $R = 0$ it is clear that an overdensity of matter, $\bar{\delta} > 0$, corresponds to a dark energy void, $\delta_\phi(R = 0, t) < 0$. Similarly, a void of matter corresponds to a local DDE overdensity at $R = 0$. In Figures 3 and 4 respectively show the
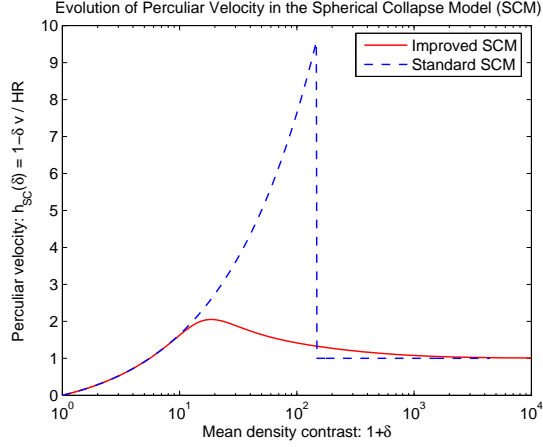
Fig. 5.— Plot showing how the peculiar velocity, $h_{SC} = 1 - \delta v/HR$, varies with the mean density contrast, $\bar{\delta}$, in both the standard spherical collapse model (dashed line) and the improved one (solid line) of Shaw & Mota (2007). The improved model is a good fit to the results of N-body simulations for $\bar{\delta} \gtrsim 15$. We note that h_{SC} reaches a maximum value of about 2 when $\bar{\delta} \approx 18$ in the improved model, whereas in the standard collapse model h_{SC} continues to grow until $\bar{\delta} \approx 140$, where it reaches a maximum value of about 9.5. In the non-linear regime, the leading order expression for $\bar{\delta}_\phi$ contains a term that is proportional to $\delta v^2 \propto h_{SC}^2$. Therefore if the standard spherical collapse model were used to evaluate δ_ϕ it could result in it being over-estimated, for $20 \lesssim \bar{\delta} \lesssim 140$, by roughly 1-2 orders of magnitude.

evolution of $\delta_\phi/(1+w)$ and $\bar{\delta}$ at $R = 0$ for a typical supercluster and a typical void. For both the supercluster and the void we assume an initial density contrast profile that is flat for $r < r_c$ and drops as $1/r^3$ for $r > r_c$. We take the initial instant to be in the far past i.e. $z_i \to \infty$. The supercluster is taken today to have a central density contrast of $\bar{\delta}(R = 0) = 2$ and $r = r_c$ to corresponds to a physical radius of $R_c = 15h^{-1}$ Mpc, which are appropriate for an object such as the local super-cluster. For the void we take typical values of $\bar{\delta}(R = 0) = -0.93$ today and $R_c = 15h^{-1}$ Mpc. In each case we have taken $\Omega_m(z = 0) = 0.27$. It is clear that in both cases $|\delta_\phi/(1+w)|$ grows faster than $|\delta_m|$, however the DDE density contrast remains much smaller than $|\delta_m|$ at all times. Note that δ_ϕ evolves monotonically for objects in both the linear and quasi-linear regimes.

5.3. Dynamical Dark Energy Clustering in the Non-Linear Regime

The quasi-linear approximation to δ_ϕ is valid for $-1 \lesssim \bar{\delta} \lesssim 10$, however it breaks down for large positive values of the matter density contrast, $\bar{\delta}$. To go further we evaluate δ_ϕ in the fully non-linear regime. To do this we need to calculate both the evolution of the peculiar velocity, δv, and that of the mean density contrast mass contrast, $\bar{\delta}$. The non-linear evolution of the matter overdensity is significantly more simple to calculate analytically in a matter dominated Universe ($\Omega_m = 1$). Fortunately, when the matter density contrast is large today $\bar{\delta} \gtrsim 100$, the evolution of both $R_{,t}$ and $\varepsilon^{(m)}$ in the inhomogeneous region are well-approximated by the $\Omega_m = 1$ solution. This is because the epoch of dark energy domination begins sometime after the cluster has turned around.

If $\Omega_m = 1$, we are effectively dealing with a Tolman-Bondi (Tolman 1934; Bondi 1947) background at leading order. We therefore have analytical solutions for R and t in terms of r and a parameter $\eta(r, t)$:

$$R = \frac{1 + \delta_i(r)}{2\delta_i(r)} r \left(1 - \cos\eta\right), \qquad (26)$$

$$t = t_s(r) + \frac{(1 + \delta_i(r))}{2H_i\delta_i^{2/3}(r)} \left(\eta - \sin\eta\right), \qquad (27)$$

where

$$t_s(r) = t_i - \frac{(1 + \delta_i(r))}{2H_i\delta_i^{2/3}(r)} \left(\eta_i(r) - \sin\eta_i(r)\right) \qquad (28)$$

$$\sim t_i \left(\frac{\delta_i(r)}{5} + \mathcal{O}(\delta_i^2)\right)$$

and

$$\eta_i(r) = \cos^{-1}\left(\frac{1 - \delta_i(r)}{1 + \delta_i(r)}\right) \sim 2\delta_i^{1/2}(r) - \frac{2}{3}\delta_i^{3/2}(r) + \mathcal{O}(\delta_i^{5/2}).$$

We assume that at early times, ($z > 1.8$), $\Omega_m \approx 1$. These solutions then provide an excellent approximation to the true early time evolution of the inhomogeneity. These solutions also provide an good approximation at late times, provided we are dealing with an overdensity of matter that turns around prior to the onset of dark energy domination ($\bar{\delta} \gtrsim 100$ today). Assuming that we are dealing with such an overdensity, we find:

$$\frac{\delta M}{R^2} = \frac{1}{2}\Omega_m H^2 R \left(\frac{9(a/a_i)^3(\eta - \sin\eta)^2}{2(t/t_i)^2(1 - \delta_t)^2(1 - \cos\eta)^3} - 1\right)$$

$$= \frac{1}{2}\Omega_m H^2 R\bar{\delta}. \qquad (29)$$

When the background is matter-dominated, $(a/a_i)^3/(t/t_i)^2 = 1$ and $\Omega_m = 1$. In the non-linear regime $\delta_t = t_s(r)/t \ll 1$, and terms proportional to δ_t in the above expression can be dropped.

We have so far modelled the matter as being a spherically symmetric, pressureless perfect fluid. This approximation neglects the random motion of the matter particles, and other effects due to the break down of spherical symmetry. These are small prior to turnaround but thereafter act to slow down the collapse of the inhomogeneity. Without any such corrections the matter perturbation would eventually collapse to a point. When these effects are included however the inhomogeneity virialises and relaxes to a steady-state. In a matter-dominated background, each shell of constant M ceases to collapse and virialises when its radius, R_{vir}, is about one half of the radius at which it turned around, R_{ta}. N-body simulations suggest that $R_{ta}/R_{vir} \approx 1.8$ (see Hamilton et al. 1991).

Since process of virialisation is not accounted for in our matter model, we must account for it in some fashion if we are to make accurate predictions. This is generally done via the rather ad hoc process of manually halting the collapse when each shell reaches its virial radius, R_{vir}; in this model one takes $R_{vir} = R_{ta}/2$; this occur at $\eta = 3\pi/2$. Whilst this provides a reasonably good approximation for the magnitude of the density contrast, $\bar{\delta}$, the peculiar velocity, δv, is discontinuous at instant of virialisation ($\eta = 3\pi/2$). This ad hoc procedure therefore gives widely inaccurate predictions for the peculiar
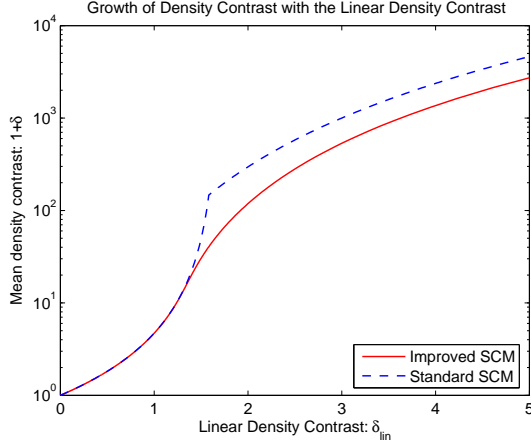
FIG. 6.— Plot showing how the true mean density contrast, $\bar{\delta}$, depends on the linear one, $\bar{\delta}_{\mathrm{lin}} \propto a(t)$ for $\Omega_m = 1$. We show both the standard spherical collapse model (SCM), the dashed line, and the improved SCM proposed by Shaw & Mota (2007), the solid line. For $15 \lesssim \bar{\delta} \lesssim 140$, the $\bar{\delta}$ grows faster in the standard SCM than in the improved one, however the overall discrepancy between the models' predictions for $\bar{\delta}(\bar{\delta}_{\mathrm{lin}})$ is not nearly as great as it is for their predictions for $h_{\mathrm{SC}}(\bar{\delta}) = 1 - \delta v/HR$: see FIG. 5.

velocity, $\delta v = R_{,t} - HR$ (see Figure 5). Since our formula for δ_ϕ depends on both δv and $\bar{\delta}$ we require a more realistic model for virialisation in the context of spherical collapse. Such an improved model was proposed recently by Shaw & Mota (2007). In this improved spherical collapse model, it is assumed that $h_{\mathrm{SC}} \equiv \delta v/HR$ is a function of $\bar{\delta}$ i.e. $h_{\mathrm{SC}} = h_{\mathrm{SC}}(\bar{\delta})$. R is still parametrized according to Eq. (26), and it is found that:

$$t = t_s(r) + \frac{(1 + \delta_i(r))}{2H_i\delta_i^{2/3}(r)}T(\tau),$$

where $\tau = \eta - \sin\eta$. The function $T(\tau)$ is then fixed so that: Prior to turnaround, when deviations from spherical symmetry are small, $T(\tau) \sim \tau$. For larger values of $\bar{\delta}$ ($\gtrsim 15$), $T(\tau)$ is chosen so that $h_{\mathrm{SC}}(\bar{\delta})$ agrees, under certain reasonable and common assumptions, with the behaviour that is seen in N-body simulations of Hamilton et al. (1991). Shaw & Mota (2007) provide the following fitting formula for $T(\eta)$:

$$T(\eta(\tau)) = \tau + \frac{3.468(\tau_f - \tau)^{-1/2}\exp\left(-\frac{15(\tau_f - \tau)}{\tau}\right)}{(1 + 0.8(\tau_f - \tau)^{1/2} - 0.4(\tau_f - \tau))}, \tag{30}$$

where $\tau_f = 5.516$. In this model $R_{\mathrm{vir}}/R_{\mathrm{ta}} \approx 0.59$ which compares more favourably with the value of 0.56 suggested by N-body simulations (Hamilton et al. 1991) than the value of 0.50 that is generally used. In this improved model, δ_ϕ is still given by Eq. 18, and for $\Omega_m = 1$ the peculiar velocity is given by:

$$\frac{\delta v}{HR} = \frac{R_{,t}}{HR} - 1 = \sqrt{\frac{1 + \bar{\delta}}{2}} \frac{\sin\eta}{(1 - \cos\eta)^{1/2}} \frac{d\tau}{dT} - 1,$$

and the density contrast is given by:

$$1 + \bar{\delta} = \frac{9T(\eta)^2}{2(1 - \cos\eta)^3}.$$

Figure 5 shows $h_{\mathrm{SC}} \equiv 1 - \delta v/HR$ as a function of $\bar{\delta}$ in both the improved spherical collapse model, and the standard one (with virialisation occurring suddenly at $R = R_{\mathrm{vir}}$). Note that in the standard spherical collapse model (SCM), h_{SC} continues to grow until $\bar{\delta} \approx 140$, and then drops sharply, whereas in the improved model h_{SC} reaches a maximum when $\bar{\delta} \approx 18$. Note also that the maximum value of h_{SC} predicted by standard SCM is almost five times as large as the maximum value gives by the improved model. Since δ_ϕ depends in part on δv^2 and hence h_{SC}^2, using the standard SCM instead over the improved model could lead to δ_ϕ being over estimated by as much as 2500%.

Figure 6 shows $\bar{\delta}$, for $\Omega_m = 1$, as a function of the mean linear density contrast, $\bar{\delta}_{\mathrm{lin}} \propto a$, in both the improved model and the standard one with virialisation put in by hand. We use our modified spherical collapse model to find the evolution of δ_ϕ. We find then that the DDE density contrast in the non-linear regime is given by:

$$\delta_\phi(R, t) \sim \frac{\Omega_m H^2(1 + w)}{2} \int_R^\infty \bar{\delta}(R', t)G(\bar{\delta}; \Omega_m)R' \, dR'$$
$$+ H^2(1 + w)R^2 h(\bar{\delta})^2, \tag{31}$$

where

$$G(\bar{\delta}; \Omega_m) = -\frac{6h(\bar{\delta})}{\bar{\delta}} + 1.$$

When $\bar{\delta} \ll 1$, $G(\bar{\delta}) \sim -1 - 2(\Omega_m^{-0.4} - 1)$, and deep in the non-linear regime, when $\bar{\delta} \gg 1$, $G(\bar{\delta}) \sim 1$. In the $\Omega_m = 1$ case we find that the following fitting formula is accurate to within 2%:

$$G(\bar{\delta}; \Omega_m = 1, \alpha = 1) \approx \tanh(-0.9218 + \tag{32}$$
$$\ln(\bar{\delta})\left(\frac{195 + 0.543\bar{\delta}^6}{403 + \bar{\delta}^6}\right) - \frac{0.38\sin^3(\ln(\bar{\delta}) - 2.49)}{(\ln(\bar{\delta}) - 2.49)^3}\right).$$

We note that when $\Omega_m = 1$, $G(\bar{\delta}) < 0$ for $\bar{\delta} \lesssim 10.6$ and is otherwise positive. In a cluster with a core overdensity $\gtrsim 20$, δ_ϕ is therefore generally positive at $R = 0$ i.e. there is DDE overdensity at $R = 0$, whereas for clusters with a core overdensity $\lesssim 10 - 20$, there is generally a DDE void around $R = 0$. Even in the deep non-linear regime, the central DDE overdensity is still surrounded by a void, with δ_ϕ becoming negative when $\bar{\delta}(R) \approx 10 - 20$. We see that $|\delta_\phi| \sim \mathcal{O}(\Omega_m(1 + w)H^2 R_c^2 \bar{\delta}/2)$, where R_c is the radius of the core of cluster (roughly defined by smallest radius after which $\bar{\delta}$ decreases faster than $1/R^2$), and $\bar{\delta}_c$ is the core density contrast i.e. the density contrast at $R = R_c$.

We use Eq. (31) to plot the evolution of $\delta_\phi(R = 0)$ in the non-linear regime. For $\bar{\delta} \gg 1$, the matter overdensity in a background with $0.2 \leq \Omega_m < 1$ evolves, to a good approximation, according to:

$$1 + \bar{\delta}(\eta)(\Omega_m) = F(a)(1 + \bar{\delta}_0(\eta)),$$

where $\bar{\delta}_0 = 9T^2/2(1 - \cos\eta)^3$ and $F(a) = \frac{4}{9t^2\Omega_m H^2} \approx \Omega^{-0.4}$. We expect the largest contributions to $\delta_\phi(R = 0)$ to come from regions where $\bar{\delta} \gg 1$ which implies that the we expect $G(\bar{\delta}; \Omega_m) \approx 1$ for all Ω_m. Therefore, using Eq. (31), we approximate:

$$\delta_\phi(R = 0, t) \approx \frac{\Omega_m^{0.6}H^2(1 + w)}{2} \tag{33}$$
$$\int_0^\infty \bar{\delta}_0(\eta)G(\bar{\delta}_0(\eta), \Omega_m = 1)R'(r, \eta)dR'.$$
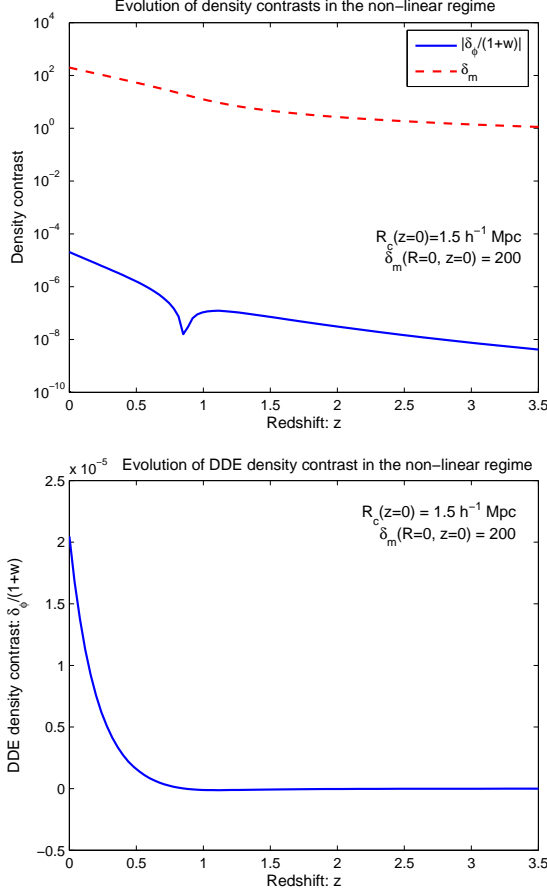
FIG. 7.— Evolution of the DDE and matter density contrasts for a cluster which today has a core matter overdensity of 200 and a core radius of $1.5h^{-1}$ Mpc. We have taken $\Omega_m = 0.27$ today. $|\delta_\phi|$ is always $\ll \delta_m$. At late times $\delta_\phi/(1 + w) > 0$, which corresponds to a central DDE overdensity, however at early times it is negative and there is a DDE void. We see that δ_ϕ changes sign when the mean core overdensity of matter is $\sim \mathcal{O}(10)$.
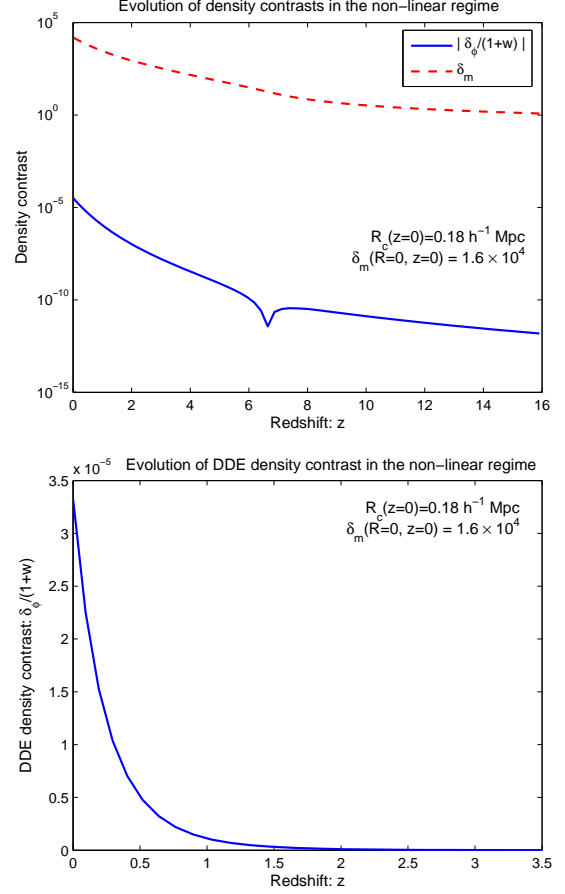
FIG. 8.— Evolution of the DDE and matter density contrasts for a cluster which today has a core matter overdensity of 1.6×10^4 and a core radius of $0.18h^{-1}$ Mpc. We have taken $\Omega_m = 0.27$ today. $|\delta_\phi|$ is always $\ll \delta_m$. At late times $\delta_\phi/(1 + w) > 0$, which corresponds to a central DDE overdensity, however at early times it is negative and there is a DDE void. We see that δ_ϕ changes sign when the mean core overdensity of matter is $\sim \mathcal{O}(10)$.

For simplicity, we take the initial density profile to have a central core with $\delta_i(r) = \delta_i$ for $r < r_c$ and for $r > r_c$, we take: $\delta_i \propto r^{-3}$.

In Figure 7 we plot $\bar{\delta}(R = 0)$ and $\delta_\phi(R = 0)$ for a cluster where today $r = r_c$ corresponds to a physical radius of $1.5h^{-1}Mpc$, and the mean density contrast in $R < R_c$ today is 200. In Figure. 8 we plot $\bar{\delta}(R = 0)$ and $\delta_\phi(R = 0)$ for a smaller but denser cluster with $R_c = 0.18h^{-1}$Mpc and $\bar{\delta}(R = 0) = 1.6 \times 10^4$ today. These values are fairly typical of clusters such as Coma which has been estimated to have a mean density contrast of 200 inside a radius of $1.5h^{-1}$ Mpc, and a core mean density contrast of about 1.6×10^4 inside a radius of $0.18h^{-1}$ Mpc. We can see that in both cases $\delta_\phi/(1 + w) \sim \mathcal{O}(10^{-5})$ today and that, as expected, it is positive. In both cases, $\delta_\phi/(1+w)$ was negative in the past, changing sign when the mean overdensity of the core was $\bar{\delta} \sim \mathcal{O}(10)$. The core in these cases corresponds to the flat part of $\bar{\delta}$ i.e. $R < R_c$. For more general density profiles, the core radius would be taken to correspond to $R \lesssim R_{-2}$ where R_{-2} is the smallest value of R for which $\bar{\delta}$ faster as R^{-2}. In all of the plots we have taken $\Omega_m(z = 0) = 0.27$.

We can see that in both cases $\delta_\phi/(1 + w)$ continues to increase today. This increase is due to the continued collapse of matter onto the collapsed core. At very late times, however, this accretion will cease, and $\delta_\phi(R = 0)/(1 + w) \rightarrow$ const for all Ω_m. We can see this from Eq. (31). At late times, and assuming minimal accretion: $\bar{\delta} = a^3\Delta(R)$, for some function $\Delta(R)$, and so:

$$\delta_\phi/(1 + w) \approx \frac{a^3\Omega_m H^2}{2} \int_0^\infty R'\Delta(R')\, dR', \qquad (34)$$

and $a^3\Omega_m H^2 =$ const which implies $\delta_\phi/(1 + w) \rightarrow$ const at late times. It is clear that $\delta_\phi/(1 + w)$ is smaller than $\bar{\delta}_{-2} = \bar{\delta}(R = R_{-2}, t)$ by at a factor of about $\Omega_m H^2 R_{-2}^2$. In follows that even at late times $\delta_\phi/(1 + w) \ll 1$, as $\delta_\phi/(1 + w) \sim \mathcal{O}(\Omega_m H^2 R_{-2}^2 \delta_{-2}) \sim \mathcal{O}(GM_{-2}/R_{-2})$, where $M_{-2} = M(R = R_{-2})$.

5.4. Discussion

We have seen that in all regimes (linear, quasi-linear and fully non-linear regimes), the magnitude of DDE density contrast scales as: $\Omega_m H^2 R_c^2 \bar{\delta}_c$, where R_c is the radial scale of the cluster, and $\bar{\delta}_c$ is the mean matter

density contrast in $R < R_c$. R_c is roughly defined to be equal to R_{-2}, which is the smallest radius for which $\bar{\delta}_c$ first decreases faster than $1/R^2$. If an inhomogeneity is sub-horizon when it begins to collapse, we found that shorter after the collapse begins $\bar{\delta}$ and δ_ϕ have the same sign i.e. a matter overdensity equates to a DDE over-density, and the same for voids. However, a certain time after collapse begins, δ_ϕ changes sign. This change of sign is related to the fact that at late times the decaying mode of the matter perturbation is negligible. When this occurs, a mean over density of matter results in a DDE void, and vice versa. Deep in the non-linear regime, when $\bar{\delta}_c \gtrsim 10 - 20$, however, $\delta_\phi(R = 0)$ changes sign again. A large mean overdensity of matter then corresponds to an overdensity of dark energy at $R = 0$.

In both the linear and the quasi-linear regimes, $|\delta_\phi/(1+w)|$ increases faster than $\bar{\delta}_c$, although it is always much smaller than $\bar{\delta}_c$. This behaviour was also observed by Dutta & Maor (2007) in their numerical study of the linear regime, and it lead them to wonder whether $|\delta_\phi/(1+w)|$ might grow to be $\mathcal{O}(1)$ or larger in the non-linear regime. Using our results, we have shown that the onset of non-linear evolution for the matter perturbation slows down the growth of $|\delta_\phi/(1+w)|$ and that at very late times $\delta_\phi/(1+w) \to$ const and remains $\ll 1$. In the next section we consider the profile of $\delta_\phi/(1+w)$ in and around typical astrophysical objects.

6. ASTROPHYSICAL APPLICATIONS

In this section we use our results to evaluate the profile of the DDE density contrast around typical clusters, superclusters and voids of matter. We also investigate the possibility of detecting the dark energy clustering using the Integrated Sachs Wolfe (ISW) effect.

6.1. *Galaxy Clusters*

We begin by considering the DDE density contrast in a virialised galaxy cluster with similar properties to the Coma cluster. Navarro, Frenk & White (1997) (hereafter NFW) used high resolution N-body simulations to derive a universal density profile for the dark-matter halos of virialised structures such as galaxies and clusters. The resulting NFW profile is given by:

$$\delta_m = \frac{\delta_c}{(R/R_c)(1 + (R/R_c))^2},$$

where R_c defines the scale at which δ_m changes from a $1/r$ drop-off to a $1/r^3$ one, and the characteristic density contrast δ_c is given by:

$$\delta_c = \frac{200}{3} \frac{c^3}{\ln(1+c) - c/(1+c)},$$

where $c = R_{200}/R_c$ defines the concentration of the halo, and R_{200} is roughly the virial radius and is defined to be the largest value of R for which the mean density contrast is ≥ 200. The mean density profile, $\bar{\delta}$, is then given by:

$$\bar{\delta} = \frac{3\delta_c(\ln(1 + R/R_c) - R_c/(1 + R/R_c))}{(R/R_c)^3}.$$

Even though $\bar{\delta} \propto 1/R$ for $R < R_c$, the integrands in Eq. (31) still behave well enough for small R for our analysis and our expression for δ_ϕ to be valid and applicable. The
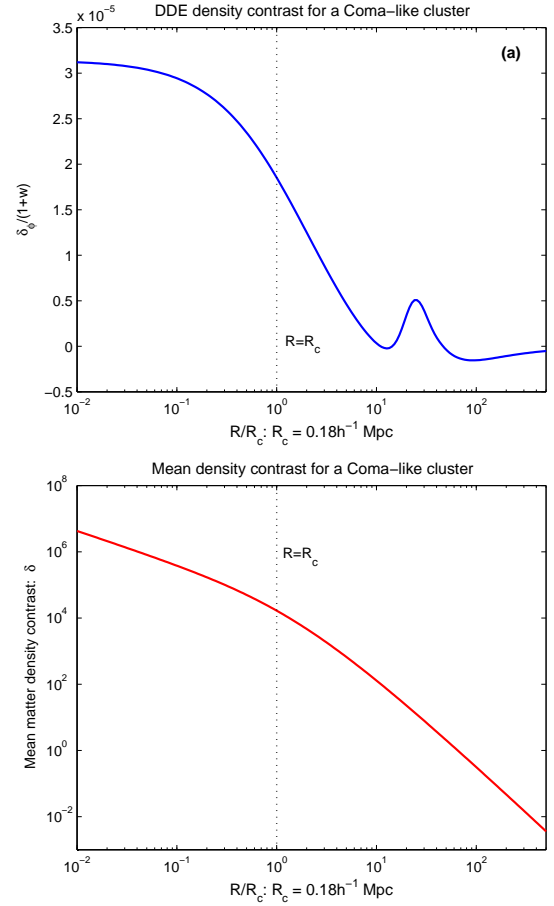

FIG. 9.— The DDE (a) and matter density (b) profiles for a Coma-like cluster with NFW profile: $R_c = 0.18h^{-1}$Mpc, $R_{200} = 1.5h^{-1}$Mpc. We have taken $\Omega_m = 0.27$. See text for discussion.

DDE density contrast in a virialised cluster is given by Eq. (31). We note that since $\delta v^2 \propto h \propto \Omega_m^{1/2}$, in the non-linear regime, and $\bar{\delta}$ depends on R only though R/R_c that, for fixed δ_c, $\delta_\phi \propto \Omega_m(1+w)H^2R_c^2$.

Geller, Diaferio & Kurtz (1999) studied the mass profile of the Coma galaxy cluster and found that over the entire range of $R < 10\,\text{Mpc}\,h^{-1}$ it increased with r at the rate predicted by the NFW profile. They found that three different observational samples were well fitted by $R_c = 0.182 \pm 0.030$, $R_c = 0.167 \pm 0.029$ and $0.192 \pm 0.035h^{-1}$Mpc with, in all cases, $R_{200} = 1.5h^{-1}$Mpc. In what follows we take R_c to be the mean of three values, $R_c \approx 0.18h^{-1}$Mpc, and $R_{200} = 1.5h^{-1}$Mpc, which corresponds to $c \approx 8.3$. We plot the profile of DDE density contrast for a Coma-like cluster in Figure 9; $R = R_c$ and $R = R_{200}$ are indicated on the plots. We have taken $\Omega_m = 0.27$ in line with WMAP (Spergel et al. 2003, 2007). We note that δ_ϕ is positive around $R = 0$ and also that it is very small $\delta_\phi(R = 0) \approx 3 \times 10^{-5}$. As R increases, δ_ϕ becomes negative when $R \approx 1.5R_{200}$, and for $R \gtrsim 4R_{200}$ it tends to 0 from below as $R \to \infty$ in line with our expectations.

6.2. *Superclusters*

Superclusters are the largest known gravitationally bound massive structures. The dark matter halos of superclusters typically have radii of about $10 - 25h^{-1}\,\mathrm{Mpc}$ and density contrasts of about $1 \lesssim \bar{\delta} \lesssim 15$. We consider two examples of such objects: the local supercluster (LSC), of which our galaxy is a part, and the Shapley supercluster (SSC) which lies about $650\,\mathrm{Mlys}$ away. The LSC has a mean overdensity of $\bar{\delta} \approx 2 - 3$ over a scale $\sim 15h^{-1}\,\mathrm{Mpc}$ (Hoffman 1986; Tully 1982). The SSC has been found to have an overdensity of $\bar{\delta} \sim 10.3$ over a scale of $10.1h^{-1}\,\mathrm{Mpc}$ (Bardelli et al. 2000). Bardelli et al. (2000) also found that if the SSC had evolved linear then it would today have a linear overdensity of $\delta_{SSC\,\mathrm{lin}} \approx 1.3$ and a linear scale of $\approx 21.6h^{-1}\,\mathrm{Mpc}$. For simplicity we model the matter density contrast of the clusters thus:

- The clusters have a homogeneous core with physical radius R_c. In $R < R_c$, $\bar{\delta} = \bar{\delta}_0$ and $\bar{\delta}_{\mathrm{lin}} = \delta_{\mathrm{lin}\,0}$.

- For $R > R_c$, the initial density contrast drops off as $1/x^3$ where $R = R_c x(1 + \bar{\delta}_0)/(1 + \bar{\delta}(R))^{1/3}$.

With this choice of density contrast, the evolution of the cluster is free from both shell-crossing and shell-focusing singularities in the linear and quasi-linear regimes. For the LSC we take $\bar{\delta}_0 = 2$ and $R_c = 15h^{-1}\,\mathrm{Mpc}$ and for the SSC we take $\bar{\delta}_0 = 10$ and $R_c = 10h^{-1}\,\mathrm{Mpc}$. We additionally considered the S300 structure, in the vicinity of the SSC, which was identified by Bardelli et al. (2000). This structure has a mean overdensity of $\bar{\delta} \approx 1.9$ on a scale of $24.8h^{-1}\,\mathrm{Mpc}$ (Bardelli et al. 2000); we take $\bar{\delta}_0 = 2$, $R_c = 25h^{-1}\,\mathrm{Mpc}$ for this structure.

We plot the DDE density contrast profile for the LSC, SSC and S300 structures in Figure 10 and Figure 11. The shape of δ_ϕ is similar for all three objects, and the magnitude of the DDE density contrast scales as $(1 + w)\bar{\delta}_0 H^2 R_c^2$; it is largest for the S300 structure and smallest for the LSC. In all three cases, it is clear that $|\delta_\phi/(1 + w)|$ is small ($\lesssim 6.2 \times 10^{-5}$) and negative which corresponds to a local DDE void,

6.3. Voids of Matter

In addition to local overdensities of matter, the Universe also contains localized underdensities of matter or voids. Voids typically have the similar radii to superclusters, although they can also be much larger. Since $|\delta_\phi/(1 + w)|$ is proportional to the square of the radius of the inhomogeneity, we expect voids to induce some of the largest DDE inhomogeneities. The classic historical example of a void is also one of the largest and was discovered in 1981 by Kirschner et al. (1981) in the constellations of Boötes and Corona Borealis. Recent measurements of this Boötes void have found it to be roughly spherical with radius $62h^{-1}\,\mathrm{Mpc}$ (Kirschner et al. 1987). 21 galaxies have been observed in the Boötes void and its mean density contrast is estimated to be: $-0.80 < \bar{\delta} < -0.66$ (Dey, Strauss & Huchra 1990). The Boötes void is particularly large and is sometimes termed a *supervoid*. Data from the 2dFGRS shows that the average radii of voids in NGP (North Galactic Pole) and in SGP (South Galactic Pole) are $14.89 \pm 2.67h^{-1}\,\mathrm{Mpc}$ and $15.61 \pm 2.48h^{-1}\,\mathrm{Mpc}$ respectively (Hoyle & Vogeley 2004; Bolejko, Krasiński & Hellaby 2005). The average mean density contrast for these voids is $\bar{\delta} = -0.94 \pm 0.02$ in
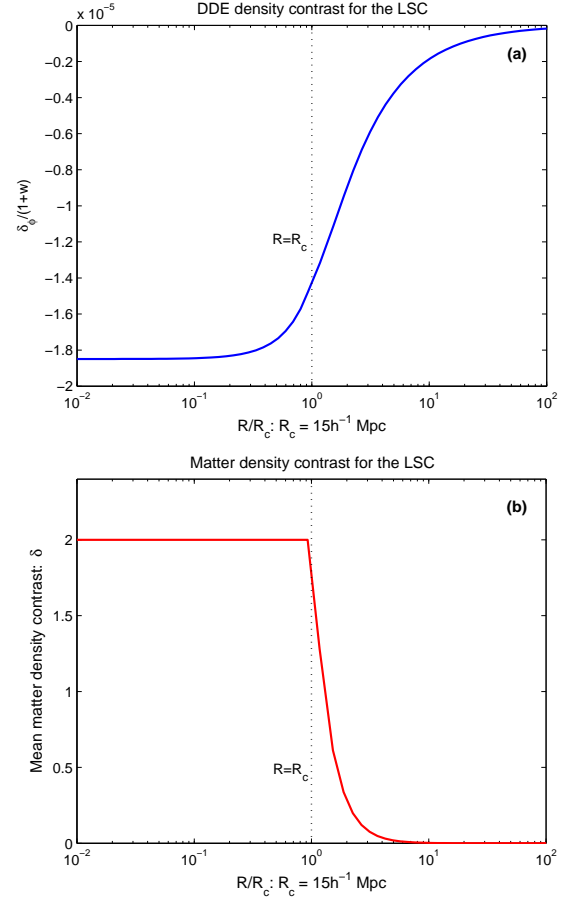

FIG. 10.— The profiles of DDE and matter density contrasts for superclusters. We have taken $\Omega_m = 0.27$. Figures (a) the DDE for the local supercluster (LSC) and Figure (b) shows our model for the LSC's matter density profile. We have taken the LSC to have a mean matter density contrast of 2 inside a radius of $15h^{-1}\,\mathrm{Mpc}$.

NGP and $\bar{\delta} = -0.93 \pm 0.02$ in SGP (Hoyle & Vogeley 2004).

Despite the large radii of these voids and supervoids, their scales are still very much sub-horizon and, as such, our results are applicable to them. The evolution of voids is well approximated by the quasi-linear regime and so we evaluate δ_ϕ using Eq. (25). We model both voids and supervoids as having a Gaussian initial mean density profile i.e. $\bar{\delta}_{\mathrm{lin}} \propto \exp(-x^2/2)$ where $R = R_c x(1+\bar{\delta}_0)/(1+\bar{\delta}(R))^{1/3}$ defines x. With this choice the evolution of the void is free from both shell-crossing and focusing singularities provided $\bar{\delta}_0 \gtrsim -0.95$.

In Figure 12 we show δ_ϕ and $\bar{\delta}$ for both a supervoid with similar properties to the Boötes void ($R_c = 62h^{-1}\mathrm{Mpc}$, $\bar{\delta}_0 = -0.75$), and Figure 13 shows the same thing but for an average void ($R_c = 15h^{-1}\,\mathrm{Mpc}$, $\bar{\delta}_0 = -0.93$). In both cases we see, as expected, that $\delta_\phi > 0$ and that a void in the matter distribution corresponds to a DDE overdensity. We note that the magnitude of $|\delta_\phi/(1 + w)|$ is an order of magnitude larger for a $60h^{-1}\,\mathrm{Mpc}$ radius supervoid than for an average $15h^{-1}\,\mathrm{Mpc}$ void. At the centre of a supervoid we see that $\delta_\phi \approx 9 \times 10^{-5}(1 + w)$, whereas at the centre of an average void $\delta_\phi \approx 5 \times 10^{-6}(1+w)$. In all cases δ_ϕ is both
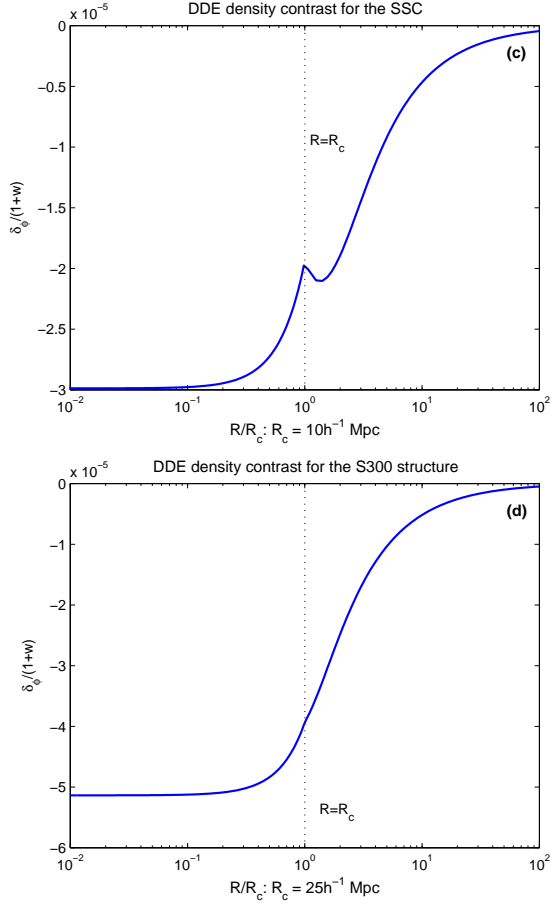
FIG. 11.— The profiles of DDE and matter density contrasts for the Shapley supercluster (SSC). We have taken $\Omega_m = 0.27$. Figure (a) shows the DDE profile for the Shapley supercluster, which has been modelled as having a mean density contrast of 10 inside a radius of $10h^{-1}$ Mpc. Figure (b) shows the DDE profile the S300 structure (with mean density contrast of 2 inside a radius of $25h^{-1}$ Mpc).
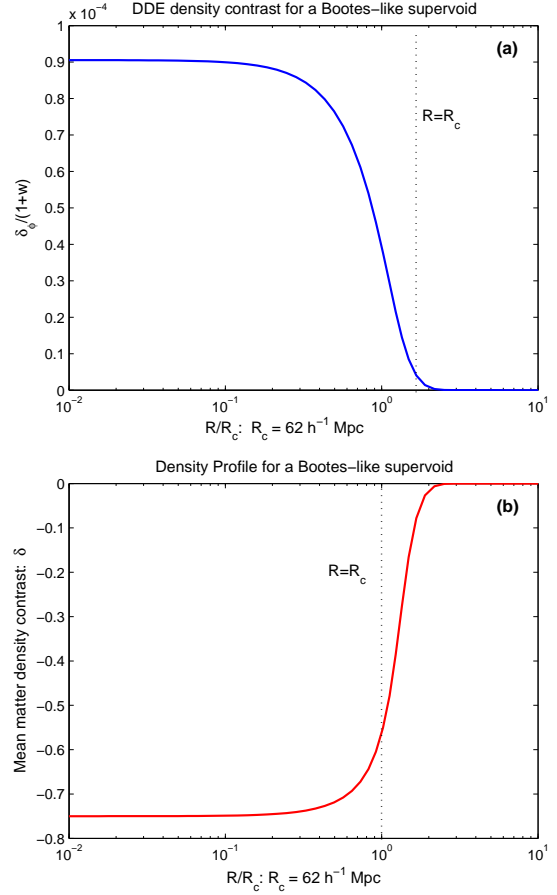
FIG. 12.— The DDE (a) and matter (b) density contrast profiles for a supervoid. We taken $\Omega_m = 0.27$ and modelled the supervoid on the Boötes void: $\bar{\delta}(0) = -0.75$ and $R_c = 62h^{-1}$ Mpc. See text for further discussion.

positive and very small.

Recently, there has been a great deal of discussion, both theoretical and observational, about the possibility that extremely large voids ($R_c \approx 100-300h^{-1}$ Mpc) exist within the visible Universe (Rudnick, Brown & Williams 2007; Inoue & Silk 2006). Additionally, a number of authors have speculated that we may even be living inside such an object (Schwarz & Weinhorst 2007; Conley et al. 2007; Zehavi et al. 1998; Giovanelli et al. 1999). For example, Rudnick, Brown & Williams (2007) showed that both the WMAP cold spot and an observed dip in the surface brightness and number counts of extragalactic radio sources could be explained by the presence of an almost completely empty $R_c \approx 105h^{-1}$ Mpc at $z < 1$. Inoue & Silk (2006) showed that the ISW effect due to a void with $\bar{\delta}_0 = -0.3$ and $R_c = 200 - 300h^{-1}$ Mpc would be observed as cold spots with a temperature anisotropy $\Delta T/T \sim \mathcal{O}(10^{-5})$, which might explain the observed large-angle CMB anomalies. If extremely large voids such as these exist they would be associated with the largest DDE overdensities within the visible Universe. In Figure 14 we plot the δ_ϕ profile for both

the $R_c = 105h^{-1}$ Mpc, $\bar{\delta}_0 \approx -1$ object postulated by Rudnick, Brown & Williams (2007) and for the $R_c = 300h^{-1}$ Mpc, $\bar{\delta}_0 \approx -0.3$ void considered by Inoue & Silk (2006). In the former case we find $\delta_\phi(R = 0)/(1 + w) \approx 2.4 \times 10^{-4}$ and in the latter $\delta_\phi(R = 0)/(1 + w) \approx 9.5 \times 10^{-4}$. These values of $\delta_\phi/(1 + w)$ are about two orders of magnitude larger than those associated with a typical void. However, even around such extremely large voids we still find that the DDE perturbation is small: $\delta_\phi/(1 + w) \lesssim 10^{-3}$.

6.4. ISW Effect due to DDE clustering

We have seen that the DDE density contrast, δ_ϕ, is always small with magnitude $\lesssim 10^{-5}$ for average sized structures in the Universe. The Integrated Sachs Wolfe (ISW) effect is highly sensitive to the presence of dark energy. In a purely matter dominated universe, the ISW effect vanishes entirely for linear perturbations. We shall see that the DDE contribution to the ISW from a cluster with radius R_c is proportional to $(HR_c)^5$ and so we consider only large (but still sub-horizon) scales. On such scales the matter perturbation is small and we are in the linear regime. The ISW effect is most easily derived in the conformal Newtonian gauge in which the metric takes
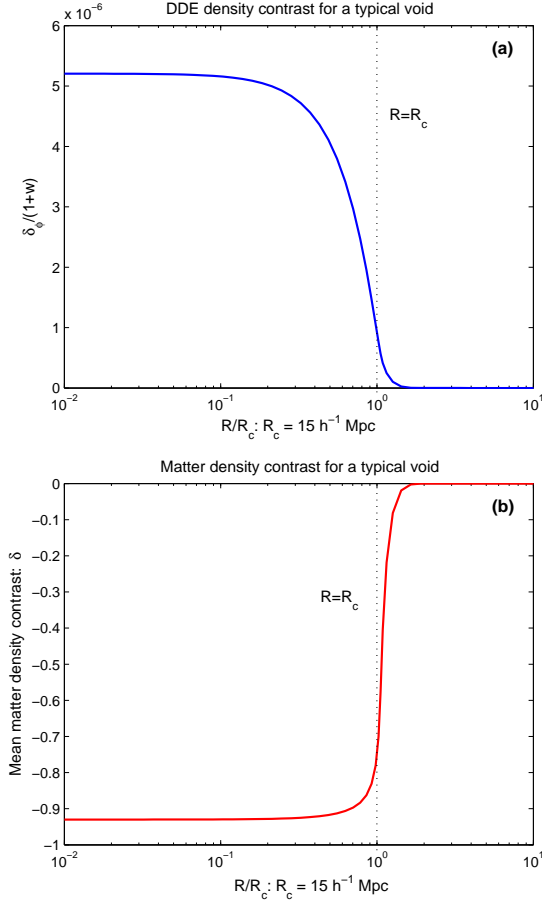
FIG. 13.— The DDE (a) and matter (b) density contrast profiles for a typical void. We have taken $\Omega_m = 0.27$ and the void to have typical properties: $\bar{\delta}(0) = -0.93$ and $R_c = 15h^{-1}$ Mpc. See text for further discussion.
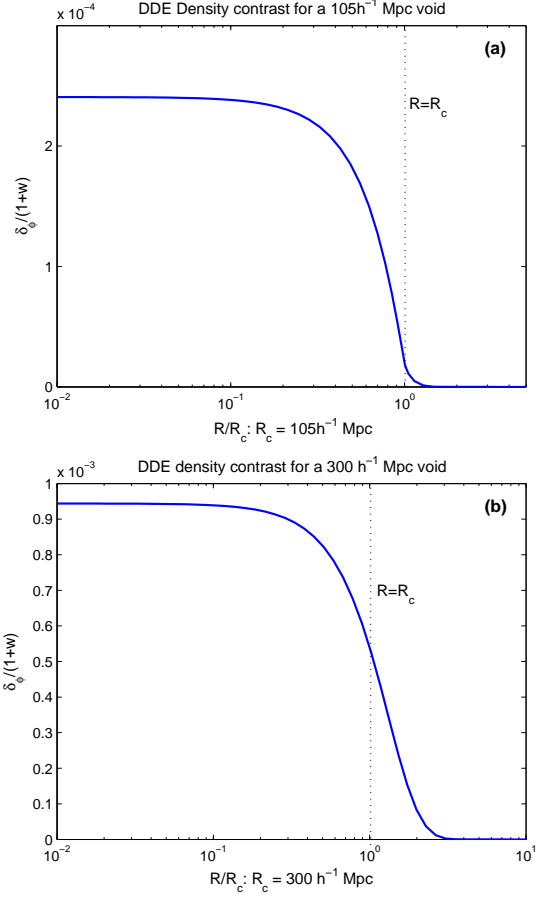

FIG. 14.— The DDE density contrast for extremely large voids. In FIG. (a) we consider a $105h^{-1}$ Mpc void with $\bar{\delta}(0) = -0.95$ and in FIG. (b) we have taken void to have radius $300h^{-1}$ Mpc and central density contrast $\bar{\delta}(0) = -0.3$. The existence of voids with these properties as recently been postulated as a mean to explain the observed large-angle CMB anomalies.

the form:

$$ds^2 = a^2 \left[(1 + 2\Psi) \, d\tau^2 - (1 - 2\Phi) \, d\mathbf{x}^2 \right].$$

Since we are dealing with shearless matter, to leading order, $\Psi = \Phi$ and, in momentum space:

$$k^2 \Phi = -\frac{3\Omega_m \mathcal{H}^2}{2} \delta_m - \frac{3(1 - \Omega_m)\mathcal{H}^2}{2}$$
$$\left(\delta_\phi + \frac{3(1 + w)\mathcal{H}^2 f(a)\delta_m}{k^2} \right) \quad (35)$$

where $\mathcal{H} = aH = \, d\ln a / d\tau$ and δ_m and δ_ϕ are defined in the rest frame of the matter particles. Using Eq. (19) we see that:

$$k^2 \Phi = -\frac{3\Omega_m \mathcal{H}^2}{2} \delta_m - \frac{9(1 + w)(1 - \Omega_m)\Omega_m \mathcal{H}^4 \delta_m}{4k^2}$$
$$= -\frac{3\Omega_m \mathcal{H}^2}{2} \left(\delta_m - \frac{(1 - \Omega_m)}{2f(a) - \Omega_m} \delta_\phi \right). \quad (36)$$

The temperature anisotropy due to the ISW effect is given by:

$$\delta_{ISW}(\hat{\mathbf{n}}) = 2 \int_{\tau_{LS}}^{\tau_0} \Phi'((\tau_0 - \tau)\hat{\mathbf{n}}, \tau) \, d\tau,$$

where τ_0 is the value of τ today and τ_{LS} is its value on the surface of last scattering and $\Phi' = d\Phi/d\eta$. The contribution to Φ' from the matter perturbation is:

$$\Phi'_m = \frac{3\Omega_m \mathcal{H}^3}{2} (1 - f(a)) \, \delta_m,$$

and $f(a) \approx \Omega_m^{0.6}$ at late times, whereas the contribution to Φ' from the DDE clustering is:

$$\Phi'_\phi = \frac{9(1 - \Omega_m)\Omega_m \mathcal{H}^5 \delta_m}{4k^4} ((1 + w)(2 + 3w - f(a)) - w_p))$$
$$= -\frac{3\Omega_m \mathcal{H}^3 (1 - f(a))}{2k^2} V(\Omega_m, w, w_p)\delta_\phi,$$

where $w_p = \, dw/ \, d\ln a$ and

$$V(\Omega_m, w, w_p) = \frac{(1 - \Omega_m)(2 + 3w - f(a) - w_p/(1 + w))}{(2f(a) - \Omega_m)(1 - f(a))}.$$

It follows that:

$$\frac{\Phi'_\phi}{\Phi'_m} \approx -\frac{3(1 + w)\mathcal{H}^2}{2k^2} \left[\frac{1 - \Omega_m}{1 - \Omega_m^{0.6}} \right]$$
$$\left(1 + \Omega_m^{0.6} + \frac{w_p}{1 + w} - 3(1 + w) \right),$$

assuming that $w_p/(1+w) \sim \mathcal{O}(1)$ or smaller in the recent past then:

$$\left|\frac{\Phi'_\phi}{\Phi'_m}\right| \lesssim \frac{3(1+w)\mathcal{H}^2}{k^2},$$

We found above that the largest DDE perturbations would mostly likely be associated with large voids of matter, with $\delta_\phi \approx 9.5 \times 10^{-4}(1+w)$ for a 300 Mpc void with central matter density contrast $\delta_0 = -0.3$ (such as that considered by Inoue & Silk 2006). In this case we would have:

$$\frac{\Phi'_\phi}{\Phi'_m} \approx -7 \times 10^{-3}(1+w)\left(1.5 - 3(1+w) + \frac{w_p}{1+w}\right),$$

which is at most $\mathcal{O}(-10^{-2}(1+w))$. In the absence of DDE clustering, the ISW temperature anisotropy of such a void was found to be $|\Delta T/T| \sim \mathcal{O}(10^{-5})$. We therefore predict that the DDE clustering contribution to the temperature anisotropy would be at most $\mathcal{O}(10^{-7}(1+w))$. For smaller objects (with radius R_c) the DDE ISW temperature anisotropy scales as R_c^4.

In conclusion: the ISW due to sub-horizon DDE clustering in models where the dark energy is due to a minimally coupled scalar field with canonical kinetic term is always suppressed by a factor of about $(1+w)(HR_c)^2$ relative to the ISW effect to the matter perturbation itself. It therefore seems unlikely that the DDE contribution detected against the background of the ISW effect caused by the matter.

6.5. *Discussion*

In this section we have applied our results to evaluate the profile and evolution of $\delta_\phi/(1+w)$ in the vicinity of typical galaxy clusters, superclusters and voids. We found that, today, the largest inhomogeneities in the DDE energy density value should occur in the vicinity of supervoids such as the one in Boötes (Kirschner et al. 1981). At the centre of a supervoid we predict $\delta_\phi/(1+w) \approx 1.6 \times 10^{-4}$. At the centre of a galaxy cluster, supercluster or average sized void, we found $|\delta_\phi/(1+w)| \approx 1 - 6 \times 10^{-5}$; with $\delta_\phi > 0$ for both virialised clusters and voids, and $\delta_\phi < 0$ for superclusters. Generally $|\delta_\phi/(1+w)| \lesssim 10^{-4}$ for supervoids, and $\lesssim 1-6\times10^{-5}$ for other structures. Recently there has been a fair amount of interest in the possibility that extremely large voids might exists with radii $R_c = 100 - 300$ Mpc. Even for objects as large as this, however, we found that $\delta_\phi/(1+w) \lesssim 10^{-3}$.

Given the current bounds on the dark energy (EoS) parameter: $w(z < 1) = -1 \pm 0.1$, our results imply that if dark energy is described by a canonical scalar field that does not couple to (or only couples very weakly to) matter and is minimally coupled to gravity, then its energy density today is virtually homogeneous with largest fluctuations no larger than 1 part in 10^5 (or possibly one part in 10^4 if 300 Mpc voids exist). Indeed, typical fluctuations in the DDE energy density will be smaller than a few parts in 10^6. We found that superclusters are generally associated with small, local DDE voids whereas most other structures (galaxies and voids of matter) are associated with local overdensities of dark energy.

7. SUMMARY AND CONCLUSIONS

In this paper we have studied how dynamical dark energy clusters over sub-horizon scales in theories where the dark energy is described by a canonical scalar field with no coupling to matter. Sub-horizon dark energy clustering in such models has always been expected to be small, but previous studies of it have assumed the matter perturbation to be small and have, for the most part relied on numerical simulations. In this paper, however, we used the powerful method of matched asymptotic expansions to derive an analytic expression, Eq. (18), for the DDE density contrast in terms of the peculiar velocity and density contrast of the matter. Our equation for δ_ϕ holds not only in the linear regime, where the matter density contrast is small, $\delta_m \ll 1$, but also in the far more interesting but far less studied quasi-linear and non-linear regimes where $\delta_m \sim \mathcal{O}(1)$ or greater.

There were then essentially two parts to this paper, finding an expression for δ_ϕ as a function of δv, δ_m and H, and then evaluating this. The evaluating part is only done approximately for models that look sufficiently like ΛCDM. So that to a first approximation we can use ΛCDM to get H, δv and δ_m. Different dark energy models would give different predictions but just from the form of δ_ϕ one can see that unless very large deviations from the ΛCDM predictions of δv, δ_m and H occur then δ_ϕ will be well approximated by taking a ΛCDM background.

Our key assumption in deriving our formula for δ_ϕ was that the matter density contrast is only $\mathcal{O}(1)$ or greater on scales that are small compared to the Hubble length, H^{-1}. This assumption holds very well for typical structures such as galaxies, clusters, superclusters and voids. We also made a number of simplifying assumptions:

- We assumed spherical symmetry. Although our interest is in dark energy rather than varying-constants, the sub-horizon dynamics of perturbations in the DDE scalar field are very similar to those of the scalar fields in varying-constant models provided one sets the matter coupling in such theories to zero. (Shaw & Barrow 2006a,b,c) studied the evolution of a light scalar field in an inhomogeneous background in the context of varying-constant. Both spherically symmetric backgrounds and ones without any symmetries were considered, and it was found that deviations from spherically symmetry did not alter the leading order behaviour of the scalar field perturbations when the matter coupling vanishes. Therefore, whilst the assumption of spherical symmetry can be relaxed, we do not expect it to greatly alter our results.

- We assumed that we were not near a black hole horizon. This assumption allowed us to take $GM/R \ll 1$ on sub-horizon scales. This assumption could also be relaxed, and once again both the form of δ_ϕ and its magnitude are not expected to be greatly effected. We again base this expectation on the results found for light scalars in the context of varying-constants by Barrow & Shaw (2007).

- We assumed that the mass of the scalar field, m, was very small compared to $1/R_c$, where R_c in the length scale of the peak in the matter density contrast. This assumption could be done away with,

however it would significantly complicate the analysis in the non-linear regime. Moreover since we have require $HR_c \ll 1$ and in most quintessence models $m \sim \mathcal{O}(H)$, it is for most models generally true that $mR_c \ll 1$. If $mR_c \sim \mathcal{O}(1)$ or larger, then we expect that it will result in a smaller DDE density contrast, i.e. smaller values of $|\delta_\phi|$.

One of the main motivations for this work was the recent work of Dutta & Maor (2007). They studied the clustering of a subclass of the DDE models which we have looked at in this work. They numerically evolved the linearized field equations for both ϕ and the metric. In the regime where the linearized equations are valid (i.e. $\delta_m \ll 1$), our analytical results agree with theirs: shortly after the collapse begins, $\delta_\phi/(1+w)$ is positive, but then as the dying mode of an overdensity of matter becomes small, $\delta_\phi/(1+w)$ changes sign and becomes negative. At late times in the linear regime an overdensity of matter corresponds to a DDE void, and vice versa. We saw in this paper that this correspondence continues to hold in the quasi-linear regime, $-1 \lesssim \delta_m \lesssim 10$, that is appropriate for superclusters and voids of matter. When $\delta_m \sim \mathcal{O}(1)$, Dutta and Maor found that $|\delta_\phi|$ could grow to be relatively large (of the order of $0.01 - 0.1$), and that this could lead to corrections to the equation of state parameter, w, of the order of a few percent. However, as we noted in the introduction, the $\mathcal{O}(1)$ values of δ_m for which this effect was found fall outside the regime where the linearized field equations which they used are actually valid. One should point out however, that in a matter dominated universe ($\Omega_m \sim 1$), there is a clear mapping between the the linear regime of an overdensity and the exact fully developed non- linear overdensity. Presumably, such mapping should occur also in the presence of a scalar field, though the multiple change of sign of the DDE perturbation complicate things considerably and this relation is not straight forward. We also saw that at late times in the linear and quasi-linear regimes $|\delta_\phi/(1+w)|$ grows faster than $|\delta_m|$. If it were not for the onset of truly non-linear behaviour in the evolution of δ_m, this would indeed lead to large values of $|\delta_\phi|$ seen at late times by Dutta & Maor (2007).

In our study we found that $\delta_\phi/(1+w)$ for realistic astrophysical objects is very small, indeed it is generally $\lesssim \mathcal{O}(10^{-4})$. The fast growth in δ_ϕ seen by Dutta & Maor (2007) for $\delta_m \sim \mathcal{O}(1)$ should therefore been interpreted as resulting from applying linearized field equations outside their realm of validity, rather than a true physical effect. Furthermore, at very late times when the matter perturbation has virialised and accretion onto the core has all but ceased, we found that $\delta_\phi/(1+w) \to$ const, and that $\delta_\phi/(1+w) \sim \mathcal{O}(GM_{-2}/R_{-2})$, where R_{-2} is the smallest radius for which $\bar{\delta}$ decreases as quickly as $1/R^2$, M_{-2} is the mass inside R_{-2}.

Whilst it is possible with highly non-linear potentials, in general it seems improbably that $O(10^{-5}(1+w))$ values of δ_ϕ, which in turn result in order $O(10^{-5}(1+w))$ values for δw will result in any pronounced non-linear effects especially over sub horizon scales. It is fair to say though that the conditions might be on the brink of breaking down for a $300h^{-1}$ Mpc void, since $HR \sim 0.1$. But for smaller objects provided the conditions we place on the potential hold (which essentially preclude small

changes in ϕ from resulting in huge changes in V, V' or V'') then there is no particular reason to think that perturbations in w will result in $O(1)$ or greater corrections to δ_ϕ. One should also point out that in the case where the scalar field is strongly coupled to matter (e.g. as in (Mota & Shaw 2006; Brax et al. 2004; Mota & Shaw 2006)), then the dark energy perturbations might not be small. Since it is natural to expect that when matter starts to infall into the nonlinear regime it will drag along the dark energy field.

We also used our analytical expression for $\delta_\phi/(1+w)$ to calculate the Integrated Sachs Wolfe (ISW) induced by the DDE density perturbations. We found that the ISW due to the DDE perturbations is always much smaller than the ISW effect due to the matter perturbation in these DDE models by a factor of roughly $\bar{H}^2 R_{-2}^2$. Indeed, even the ISW effect due to the clustering of DDE near an extremely large 300 Mpc is found to result in a temperature anisotropy no larger than $\mathcal{O}(10^{-7}(1+w) \lesssim 10^{-8})$. For smaller objects the ISW effect due to DDE clustering scales as R_c^4 (where R_c is the radius of the cluster). It is therefore unlikely that, if dark energy is described by a simple uncoupled quintessence theory, DDE perturbations will be detected through the ISW effect.

In summary: we have derived an analytical expression for the DDE density contrast in uncoupled quintessence models and used it to make quantitative predictions for DDE clustering. Our results should also apply to fields with very weak matter coupling. This analysis could also be straightforwardly extended to models that are coupled to matter but we leave this to a later work. If the mass of the scalar in these models is $\mathcal{O}(H)$, then $\delta_\phi/(1+w)$ is, to leading order, independent of the specifics of the underlying theory. As opposed to what has been suggested elsewhere, we found that $\delta_\phi/(1+w)$ is always small compared to the matter density contrast, and that even when the matter perturbation goes non-linear, $\delta_\phi/(1+w)$ remains $\lesssim 10^{-3}$ for typical astrophysical objects. If we define the radius, R_c, of a matter over/under - density by the condition that at $R = R_c$, the mean matter density contrast drops off like $1/R^2$, then we found that $|\delta_\phi/\bar{\delta}| \sim \mathcal{O}((1+w)H^2R_c^2)$. DDE clustering could potentially be detected through the ISW effect or measurements of the peculiar velocity field of matter. Roughly, the magnitude of the DDE clustering contribution to these effects is a factor $|(1-\Omega_m)\delta_\phi/\Omega_m\delta_m| \sim \mathcal{O}((1-\Omega_m)(1+w)H^2R_c^2/\Omega_m) \ll 1$ times the contribution from the clustering of ordinary matter. For realistic astrophysical objects, we found that voids and super-voids correspond to local overdensities in dark energy, with $\delta_\phi/(1+w) \sim \mathcal{O}(10^{-5})$ for clusters and average voids, and $\delta_\phi/(1+w) \sim \mathcal{O}(10^{-4})$ for super-voids. If voids with radii of $100 - 300$ Mpc exist within the visible Universe then δ_ϕ may be as large as $10^{-3}(1+w)$. Linear overdensities of matter and super-clusters generally correspond to local voids in dark energy; for a typical super-cluster: $\delta_\phi/(1+w) \sim \mathcal{O}(-10^{-5})$.

Astronomical observations indicate $w = -1 \pm 0.1$ for $z < 1$, and so we conclude that if dark energy is described by an uncoupled quintessence model, then today dark energy is almost homogeneous on sub-horizon scales with perturbations generally of order of 10^{-6}; the largest perturbations will be $\mathcal{O}(10^{-5} - 10^{-3})$ and associated with

very large voids of matter.

REFERENCES

Abramo L. R., Batista R. C., Liberato L. and Rosenfeld R. (2007), `arXiv:0707.2882 [astro-ph]`.

Adelman-McCarthy J. K. *et al.* (2006), Astrophys. J. Suppl. **162** 38.

Amendola L. (2000), Phys. Rev. D **62**, 043511.

Amarzguioui M., Elgaroy O., Mota D. F. and Multamaki T. (2006), Astron. Astrophys. **454** 707.

Balaguera-Antolínez A., Mota D. F. and Nowakowski M. (2006), Class. Quant. Grav **23**, 4497-4510.

Balaguera-Antolínez A., Mota D. F. and Nowakowski M. (2007), to appear in Mon. Not. Roy. Astro. Soc..

Bardelli S., Zucca E., Zamorani G., Moscardini L. and Scaramella R. (2000), Mon. Not. Roy. Astro. Soc. 312, 540.

Barrow J. D. and Shaw D. J. (2007), Gen. Rel. Grav. to appear in Obregon's Festschrift.

Bartelmann M., Doran M. and Wetterich C. (2005), `[arXiv:astro-ph/0507257]`.

Bondi H., Mon. Not. R. astron. Soc. **107**, 410 (1947)

Bolejko K., Krasiński A. and Hellaby C. (2005), Mon. Not. Roy. Astron. Soc. 362, 213.

Brax et al. 2004 Phys.Rev.D70, 123518.

Brookfield A. W. *et al.* (2006), Phys. Rev. Lett. **96**, 061301.

Brookfield A. W., van de Bruck C., Mota D. F. and Tocchini-Valentini D. (2006b), Phys. Rev. D **73**, 083515.

Caimmi R., 2007, New Astron.12:327-345.

Capozziello S., Cardone V. F. and Troisi A. (2005), Phys. Rev. D **71**, 043503.

Conley A. *et al.* (2007), `arXiv:0705.0367 [astro-ph]`;

Corasaniti P., Giannantonio T and Melchiorri A. (2005), Phys. Rev. D **71**, 123521.

Dey A., Strauss M. A. and Huchra J. (1990), Astron. J. 99, 463.

Doran M., Robbers G. and Wetterich C. (2007), Phys. Rev. D **75**, 023003.

Dutta S. and Maor I. 2007, Phys. Rev. D **75**, 063507.

Dvali G. R., Gabadadze G. and Porrati M. (2000), Phys. Lett. B **485**, 208.

Geller M. J., Diaferio A. and Kurtz M. J. (1999), Astrophys. J. 517, L23.

Giovanelli R. *et al.* (1991), Astrophys. J. 525 25.

Hamilton A. J. S., Kumar P., Lu E., Mathews A. (1991), Astrophys J., 374, L1.

Hannestad S. and Mortsell E. (2002), Phys. Rev. D **66**, 063508.

Hinch E. J. (1991), *Perturbation methods*, (CUP, Cambridge).

Hoyle F. and Vogeley M. S. (2004), Astrophys. J. 607, 751.

Hoffman Y. (1986), Astrophys. J. 308, 493.

Inoue K. T. and Silk J. (2006), `[arXiv:astro-ph/0612347]`

Kirschner R. P., Oemler A., Schechter P. L. and Shectman S. A. (1981), Astrophys. J. 248, L57.

Kirschner R. P., Oemler A., Schechter P. L. and Shectman S. A. (1987), Astrophys. J. 314, 493.

Koivisto T. and Mota D. F. (2006), Phys. Rev. D **73**, 083502 [arXiv:astro-ph/0512135].

Koivisto T. and Mota D. F. (2007a), Phys. Lett. B **644**, 104 (2007).

Koivisto T. and Mota D. F. (2007b), Phys. Rev. D **75**, 023518 (2007).

Kolb E., Matarrese S. and Riotto A. (2006), New J.Phys. 8 322.

Lahav O. *et al.* (1991), Mon. Not. Roy. Astro. Soc. 251 128.

Linder E. and White M. (2005), Phys. Rev. D **72**, 061304.

Mainini R. (2005), Phys. Rev. D **72**, 083514.

Manera M. and Mota D. F. (2006), Mon. Not. Roy. Astron. Soc. **371** 1373 `[arXiv:astro-ph/0504519]`.

Moffat J. W. (2006), J. Cosmol. Astropart. Phys. 05.

Maor I. and Lahav O. (2005), `[arXiv:astro-ph/0505308]`.

Mota D. F. and van de Bruck C.(2004), Astron. Astrophys. **421**, 71.

Mota D. F., Shaw D. J., 2006, Phys.Rev.Lett. 97, 151102

Mota D. F., Shaw D. J. ,2007, Phys. Rev. D 75, 063501

Navarro J. F., Frenk C. S. and White S. D. M. (1997), Astrophys. J. 490, 493.

Nojiri S. and Odintsov S. D. (2003), Phys. Rev. D **68**, 123512.

Nunes N. J. and Mota D. F. (2006), Mon. Not. Roy. Astron. Soc. 368:2 751 `[arXiv: astro-ph/0409481]`.

Nunes N. J., da Silva A. C. and Aghanim N. (2005), `[arXiv:astro-ph/0506043]`.

Peebles P. J. E. and Ratra B. (1998), ApJ **325**, L17.

Peebles P. J. E. (1980), The large scale structure of the Universe, Princeton University Press.

Pettorino V., Baccigalupi C. and Mangano G. (2005), JCAP **0501**, 014.

Percival W. J. (2005), `[arXiv:astro-ph/0508156]`.

Perlmutter S. *et al.* (1999), Astrophys. J. **517**, 565.

Riess A. G. *et al.* (1998), Astron. J. **116**, 1009.

Riess A. G. *et al.* (2004), Astron. J. **607**, 665.

Riess A. G. *et al.* (2006a), to appear in Astrophys. J.

Riess A. G. *et al.* (2006b), `[arXiv:astro-ph/0611572]`.

Rudnick L., Brown, S. and Williams L. R. (2007), `arXiv:0704.0908 [astro-ph]`

Schwarz D. J., Weinhorst B. (2007), `arXiv:0706.0165 [astro-ph]`;

Shaw D. J. and Barrow J. D. (2006a), Phys. Rev. D 73, 123505.

Shaw D. J. and Barrow J. D. (2006b), Phys. Rev. D 73, 123506.

Shaw D. J. and Barrow J. D. (2006c), Phys. Lett. B 639, 596.

Shaw D. J. and Mota D. F. (2007), to appear in Astrophys. J. Supp.

Spergel D. *et al.* (2003), Astrophys. J. Suppl. **148**, 175.

Spergel D. *et al.* (2007), Astrophys. J. Suppl. **170**, 377.

Tegmark M. *et al.* (2006), Phys. Rev. D **74** 123507.

Tolman R. C. (1934), Proc. Nat. Acad. Sci. USA 20, 169.

Tully R. B. (1982), Astrophys. J. 257, 389.

Wang P. (2006), Astrophys. J. **640**, 18.

Wang L. and Steinhardt P. (1998), Astrophys. J. **508**, 483.

Weller J. and Lewis A. M. (2003), Mon. Not. Roy. Astron. Soc. **346**, 987.

Wetterich C. (1988), Nucl. Phys. **B302**, 668.

Wood-Vasey W. M. *et al.* (2007), `astro-ph/0701041`.

Zehavi I. *et al.* (1998), Astrophys. J. 503 483.